# Review of BWR Fuel Failures and Degradation From 1993 to Early 2000

1000692

# Review of BWR Fuel Failures and Degradation From 1993 to Early 2000

**1000692**

Technical Progress, September 2000

EPRI Project Manager
B. Cheng

EPRI • 3412 Hillview Avenue, Palo Alto, California 94304 • PO Box 10412, Palo Alto, California 94303 • USA
800.313.3774 • 650.855.2121 • askepri@epri.com • www.epri.com

## DISCLAIMER OF WARRANTIES AND LIMITATION OF LIABILITIES



ORGANIZATION(S) THAT PREPARED THIS DOCUMENT

**ANATECH Corp.**



## ORDERING INFORMATION

Requests for copies of this report should be directed to the EPRI Distribution Center, 207 Coggins Drive, P.O. Box 23205, Pleasant Hill, CA 94523, (800) 313-3774.

# CITATIONS

---

This report was prepared by

ANATECH Corp.
543D5 Oberlin Drive
San Diego, CA 92121

Principal Investigator
D. Sunderland

This report describes research sponsored by EPRI.

The report is a corporate document that should be cited in the literature in the following manner:

*Review of BWR Fuel Failures and Degradation From 1993 to Early 2000,* EPRI, Palo Alto, CA: 2000, 1000692.

# EPRI PERSPECTIVE

Secondary degradation of failed rods was a major concern for BWR utilities during the late 1980s and the first half of 1990s, because of wide-spread experience of long axial cracking of the then common cladding type containing a high purity zirconium liner. The long axial cracking of the cladding often resulted in washout of significant quantities of irradiated fuel pellets into the reactor water. Low corrosion resistance of the high purity zirconium liner in steam has been considered as a contributing factor to the secondary degradation. Two BWR fuel suppliers introduced alloyed-liner containing either Fe or Sn to improve the corrosion resistance of the liner in the early 1990s. The third BWR fuel supplier introduced an alloyed liner containing Fe during the second half of 1990s. Some utilities have elected to use non-barrier cladding. Improvements in cladding material may have contributed to the decreased frequency and severity of secondary degradation. However, diligent use of in local power suppression by utilities and control of power changes while operating failed rods may have played an import role in the current success.

There have been other changes in the 1990s. First of all, the rate of primary failure due to debris fretting has been decreasing through the 1990s as new fuel has incorporated debris-resistant bottom tie plates (nozzles) and utilities have implemented foreign material exclusion or debris mitigation programs. These factors are significant since the majority of severe degradation cases are associated with debris fretting failures. Secondly, the fuel lattice design has been changed to predominantly 9x9 and 10x10 from the 8x8 design, which dominated the previous decade. Another factor is the emergence of circumferential cracking, which is a form of severe localized hydriding, in some high duty, failed rods.

The objective of this project is to assess the post-failure performance of 9x9 and 10x10 fuel designs with non-barrier and different alloy-liners and to develop trends that describe the propensity of different BWR cladding types to experience secondary degradation with either axial or circumferential cracking. A total of 172 failures, which occurred in cycles ending since 1993, have been surveyed. However, detailed information on the degradation condition was obtained on only 100 failed rods. Although the database is still too limited to allow establishing clear trends in some cases, particularly relating to the new alloy liners, some interesting observations can be made. These include a correlation of predominant debris failure sites at spacers 4-7 and degradation, absence of an effect of lattice design on degradation propensity, and different propensities of barrier and non-barrier rods to develop axial and circumferential cracking. Currently, only 5 out of 13 failed alloy liners (4 Zr-Sn liner and 1 GE Zr-Fe liner) have been assessed regarding to degradation. All 5 rods exhibited moderate hydriding, and none experienced either axial or circumferential cracking. To evaluate whether the alloy liners are more resistant to degradation, future assessment should include comparing the local power histories of the failed alloy liner rods with that which would induce severe secondary degradation in barrier cladding.

# CONTENTS

# LIST OF FIGURES

# LIST OF TABLES

# 1 INTRODUCTION

Although the occurrence of LWR fuel failures has declined in frequency, fuel failures are a persistent problem for nuclear utilities operating Boiling Water Reactors (BWR's). Primary failure mechanisms such as PCI and CILC, which plagued the industry during the 1970's and 1980's, have been overcome with improved fuel rod and cladding designs. The primary cause of BWR fuel failures since the late 1980's has been debris fretting, and a small population of failures has been attributed to manufacturing defects.

One remedy for PCI was the use of a soft, chemically pure zirconium layer metallurgically bonded to the inside surface of the cladding. The zirconium liner (or barrier) increased the resistance of the cladding to stress corrosion cracking by iodine or cesium. However, a disadvantage of this design is the lack of corrosion resistance in the presence of water or steam, following primary failure of the fuel rod. The pure Zr-liner has been implicated as a contributing factor in the secondary degradation (physical damage, such as long axial cracks, and excessive radioactivity release) of many BWR failures. In response to this, BWR fuel manufacturers have introduced alloy liner fuel in which the pure Zr-liner has been replaced with Zr-alloy liners containing alloying elements Sn or Fe to increase the liner corrosion resistance. Another development in degradation resistant cladding is a triple layer design (Zr-2/Zr/Zr-2) in which a thin layer of corrosion resistant Zr-2 is overlaid on the inside of the cladding thus protecting the less corrosion resistant Zr layer while maintaining the PCI resistance of the Zr material.

Another trend in the BWR community is the acceptance of fuel assembly designs with higher order lattices, e.g. 9x9 and 10x10. In general, the local power level decreases with the higher order lattices, reducing the mechanical demands on the cladding. These designs may also incorporate the alloy liner cladding. However, in order to avoid the risk of severe secondary degradation with failed fuel, some utilities are returning to non-barrier fuel in higher order lattices, particularly 10x10 fuel. This approach imposes the use of restrictive operating practices in which power ascension rates are limited and control blade movements are performed at reduced core power in order to minimize cladding stresses.

Since these design changes have been introduced, there have been approximately 48 failures in 10x10 fuel, with ten (10) failures in cladding with alloy liner. While the occurrence of long axial splits has diminished, many of the 10x10 failures seem susceptible to localized massive hydride damage resulting in circumferential fractures or loss of cladding material over the length of 2 or 3 fuel pellets (1-2 inches, 25-50 mm). Approximately 60 failures have occurred in 9x9 fuel, both barrier (non-alloy liner) and non-barrier, with some indication that non-barrier cladding is less susceptible to secondary degradation.

In order to evaluate the effectiveness of new fuel designs to mitigate secondary degradation, it is important to collect and review the performance of current (post-1993) fuel rod failures. Comparison of operating conditions, off-gas release, and physical appearance of current fuel rod failures and past experiences with secondary degradation can provide insight into the impact of design or operating changes introduced to improve post primary failure performance. The principal objectives of this project are to assess the post-failure performance of 9x9 and 10x10 fuel designs with non-barrier and alloy-liner cladding and to develop trends that describe the propensity of BWR cladding to experience secondary degradation. Such an understanding can assist utilities in making more informed decisions during fuel design evaluations and when operating with failed fuel.

This report contains the results of a survey of 172 failed fuel rods, from cycles which concluded since 1993 (although 4 fuel rods were included from cycles ending in 1992 because they involved non-barrier 8x8 or early 9x9 non-barrier, and two rods were removed during a mid-cycle outage in 1992). Regarding the dates, the objective here is to review failures in more modern fuel and compare with previous experience observed in mostly 8x8 fuel with or without sponge liner.

The report summarizes the trends in secondary degradation with:

- Alloy-liner and Non-barrier vs. Barrier (Pure Zr-liner) fuel
- Primary Failure Modes and Secondary Degradation Type in 9x9 and 10x10 fuel
- Suppressed vs. non-suppressed (low and high power) fuel
- Low vs. high burnup fuel
- Time of operation with primary defect

Distance Between Primary Defect and Secondary Degradation

# 2
# SUMMARY OF THE DATABASE

## 2.1Structure of the Database

The database contains 172 cases of failed BWR fuel rods, which have occurred since 1993 in BWRs operating in the US, Europe, and Asia. The fuel designs from three manufacturers are represented as follows:

ABB: 54 fuel rods

GE: 77 fuel rods

Siemens/SPC: 41 fuel rods

The distribution among the designs, according to lattice order and barrier/non-barrier cladding are provided in Table 2-1. The majority (84%) of 8x8 failures has occurred in barrier cladding, while two-thirds of the failures in 9x9 population and only 25% of the 10x10 failures have barrier cladding. All of the ABB barrier fuel in the database has the Zr-Sn alloy-liner, while the GE and Siemens barrier failures have a pure Zr-liner. These statistics reflect the fact that much of the 10x10 fuel in operation has incorporated non-barrier cladding.

**Table 2-1**
**Distribution of Fuel Designs in the Database**

| Vendor | Cladding | 8x8 | 9x9 | 10x10 | Totals |
|---|---|---|---|---|---|
| ABB | Barrier (alloy) | 1 | - | 11 | 12 |
| | Non-barrier | 8 | - | 34 | 42 |
| GE | Barrier (Zr) | 49 | 27 * | 1 | 77 |
| | Non-barrier | - | - | - | - |
| Siemens | Barrier (Zr) | 3 | 15 | - | 18 |
| | Non-barrier | 2 | 19 | 2 | 23 |
| Totals | | 63 | 61 | 48 | 172 |

* Includes 1 Zr-Fe Liner failure

The database is provided in an Excel Spreadsheet format. The data are grouped by fuel manufacturer and then arranged chronologically by the cycle-end date. The data provided in the database include the following categories:

- Unit, Cycle, Dates
- Fuel assembly, Assy. ID, Rod Location, Fuel Design, Discharge Burnup
- Cause of Primary Failure, Time/Burnup of Primary Failure, Location and Type of Primary Defect and Secondary Degradation
- Operating Conditions: Power at failure and after suppression, plant operation and water chemistry
- Off-gas and Coolant Activity

The individual categories are provided in Table 2-2. The unit, cycle and dates of operation were readily available from the utilities and other open literature sources. The fuel assembly identification, rod location, fuel design and discharge burnups were also obtained from utilities. Less readily available were the location and type of secondary degradation, and in several cases where the fuel could not be inspected due to significant damage, the primary location was not identified.

While general plant operating conditions, such as type of core operation, spectral shift and water chemistry, were readily available from most utilities, detailed off-gas and coolant activities were more difficult to obtain. The power of the fuel rods, both before and after suppression (if the latter was applied), proved the most difficult to obtain.

Of the 172 cases in the database, details of the secondary degradation type and location were provided for 100 cases. Of these cases, rod average power at the time of failure and after suppression, if applied were obtained for 20 cases. Detailed axial power shapes at the time of failure were provided for 4 cases and following suppression in one of these cases.

**Table 2-2**
**Data Entries for BWR Fuel Failure Degradation Database**

1. Reactor
2. Cycle
3. BOC date
4. EOC date
5. Assembly Id
6. Rod location (lattice position)
7. Cause of failure (e.g. debris, PCI, etc)
8. Fuel design
9. Burnup at Failure, GWD/MTU (estimated)
10. Burnup at Discharge, GWD/MTU
11. Date of failure
12. Date of discharge
13. Location of primary defect
14. Location of secondary damage
15. Cladding type (V = vendor information)
16. Clad. Fabrication date (V= vendor information)
17. Date of first operation of fuel
18. Date of flux tilt and CRB insertion (Power Suppression Test)
19. No. CRBs inserted
20. Flux Tilt - Reactor Power
21. Rod Avg. LHGR at failure
22. Rod Avg. LHGR after suppression
23. Plant water chemistry (NWC, ZnWC, HWC, NMCA)
24. Core operation (CCC=control cell core, ILLCD, CNV=conventional core, M = monosequence
25. Core flow (e.g. MEOD, MELLA, ELLLA)
26. Spectral Shift (Y or N)
27. Minimum Flow (% of Full Rated Flow)
28. Power level for Control Rod Movement (withdrawal)
29. Frequency of Deep-Shallow Control Blade Exchange (Rod Swap) and Pattern Adjustments (Reactivity Adjustments)
30. Core power ramp rate (e.g. %/hr, kW/ft-hr, kW/m-hr) or Fuel ramp rate restrictions

Steady-state (average) before failure (background off-gas):

31. Σ6 Off-gas (SJAE)
32. Coolant activity, I-131
33. Coolant activity, DEI
34. Coolant activity, Np-239

Steady-state (or maximum) after failure but before suppression:

35. Σ6 Off-gas (SJAE)
36. Coolant activity, I-131
37. Coolant activity, DEI
38. Coolant activity, Np-239

Steady-state (or maximum) after suppression (if applicable):

39. Σ6 Off-gas (SJAE)
40. Coolant activity, I-131
41. Coolant activity, DEI
42. Coolant activity, Np-239
43. Estimated fuel loss (g $UO_2$)

## 2.2 Description of Primary Failure and Secondary Degradation

### Primary Defects

The primary defect is identified in terms of the cause, e.g. Debris, Unk (for unknown), PCI, Mfg (for manufacturing-related) and CILC, and by the location (elevation) of the primary defect. In the case of debris, in addition to elevation, the spacer grid number is provided. The distribution of debris as a function of spacer number is given in Table 2-3. The lowest spacer is spacer 1 (Sp 1) and the uppermost spacer is Sp 6, 7 or 8 depending on the design (S64 and S100 designs have 6 spacers; S96 has 7 spacers). Of the 62 confirmed debris failures, 77% of the failures occur in the spacers 4 through 7.

**Table 2-3**
**Distribution of Debris Failures**

| Vendor | LEP | Sp 1 | Sp 2 | Sp 3 | Sp4 | Sp5 | Sp6 | Sp7 | **Sp8** (GE13, GE12/14, SV96 Opt, ATR10) |
|---|---|---|---|---|---|---|---|---|---|
| A | 4 | - | - | - | 3 | 8 | 11 | 1 | |
| G | 3 | - | - | - | 4 | 1 | 4 | 10 | |
| S | 5 | 2 | - | - | 4 | 2 | 1 | 1 | |
| Total | 12 | 2 | - | - | 11 | 11 | 16 | 12 | |

This database confirms that debris has been a persistent problem in the industry as is evident by the fact that the majority of failures (88 of 172 failures) are failed by debris. The distribution among the fuel designs from three manufacturers are represented as follows:

ABB: 54 fuel rods (42 Debris Confirmed - 78%)

GE: 77 fuel rods (25 Debris Confirmed - 32%)

Siemens/SPC: 41 fuel rods (21 Debris Confirmed - 51%)

There are several failures for which the cause of failure is unknown or not provided, partly due to limitations with the inspection as a result of the degradation, and several of these could be debris failures.

With regard to the unknown (Unk) classified failures, there are a number of cases in which a probable cause is suspected, although further detailed inspection would require removal of the fuel rod from the assembly, and possibly PIE at the hot cell. In these cases, the suspect cause is provided with the Unk classification, e.g. Unk-Mfg (where a manufacturing defect such as a fuel pellet or cladding defect is responsible for a PCI-type failure mechanism, designated PCI-2) or Unk-PCI (where the classic PCI mechanism may be indicated).

There are 19 failures in barrier fuel in which the classification is "Unk-Mfg, PCI-2". Another case is designated as PCI-2 since it has been confirmed that there is missing pellet surface adjacent to the primary defect site [Ref 1, 2]. All of these cases in this database occurred during the years 1993-1996, and the failures occurred in fuel which was manufactured during a certain period of time in which certain pellet and cladding defects were known to have occurred. There were other similar cases which occurred in the years prior to 1993, and which are not included in database. The reason for the "Unk" designation is the lack of confirmation of evidence of missing pellet surface or a cladding flaw, which would be damaged by degradation.

PCI, i.e. the classic PCI mechanism, has occurred in a limited number of non-barrier fuel failures of older 8x8 and 9x9 fuel designs. In the 8x8 fuel, PCI was attributed to high power operation following a control blade withdrawal after long periods of controlled lower power operation. This type of operation is also believed to be a contributing factor to a number of failures in 8x8 barrier fuel, possibly in conjunction with some manufacturing defect such as missing pellet surface or an undetected cladding flaw. In some 9x9 non-barrier fuel, which experienced PCI, the vendor concluded that pellet chips in the fuel-cladding gap promoted high cladding stresses, which led to failure. PCI in 9x9 non-barrier fuel, certainly does not require pellets chips, but will occur under appropriate power ramps even for pellets of good manufactured quality.

There are several types of manufacturing (Mfg) failures, other than the missing pellet surface (PCI-2) and cladding flaws which were implicated in a number of 8x8 barrier failures during the early and mid-1990’s. Two endplug weld defects were reported, one in 1994 and one in 1996. Endplug welds may lead to failure through the propagation of a defect associated with an inclusion or sharp notch, or due to local corrosion. These type of defects are quite rare.

Crud-induced localized corrosion of the type that occurred during the 1970’s and early 1980’s has been eliminated as a cause of failure through improvements in cladding design and primary water chemistry. However, there was a recent event at one plant in 1999 where a number of assemblies developed significant deposits of crud, which then lead to failure due to accelerated corrosion on high power fuel rods. This type of crud related corrosion is designated CILC-II to distinguish it from the older classic CILC. In the recent CILC-II case, the cladding was highly resistant to nodular corrosion.

### *Secondary Defects and Degradation*

Secondary defects and the degradation are described in terms of the type and location (elevation) along the fuel rod. The following codes are used to describe the type of degradation in order of severity and are based on utility summary reports:

Severe Degradation (Category 4 - Off-gas (Xe, Kr) and iodine activities, and release of significant fuel particles (> 2 gm of fuel)):

- cr = crack (Severe Type 1 - crack length > 6 inches)
- cf = circumferential fracture (Severe Type 2 - if guillotine break separates, or local loss of cladding)

Major Degradation (Category 3 - Off-gas (Xe, Kr) and iodine activities, and small release of fuel particles (1-2 gm of fuel)):

- cr = crack (crack length < 6 inches)
- cf = circumferential fracture (partial break or tight guillotine)

Moderate Degradation (Category 2 - Off-gas (Xe, Kr) and low to moderate iodine activities):

- bls = blister
- crblg = cracked bulge
- blg = bulge

Minor Degradation (Category 1 - Off-gas (Xe, Kr) and slight iodine activity - mostly from primary site):

- hyd = hydride (surface discoloration - no physical damage)
- ec = eddy-current indication

The term "cr" refers to axial or longitudinal cracks, as opposed to circumferential or transverse cracks "cf". In some infrequent cases, a crack has a spiral orientation, traveling longitudinally and circumferentially (azimuthally) around the cladding tube. These types of defects, examples of which are provided in Figure 2-1, are considered major or severe degradation, since loss of fuel to the coolant will occur. An example of a severe form of degradation is provided in Figure 2-2, in which the hydriding has progressed beyond a circumferential crack or axial crack into massive local hydriding. In this figure, approximately 1-2 inches of cladding has disintegrated and the pellets at this location have oxidized and washed out.

The remaining terms refer to forms of secondary hydriding and reflect the terminology of the observers. Bulges ("blg") and blisters ("bls") indicated raised areas of the cladding outer surface. A blister is a ruptured bulge in which the hydriding is so severe that the cladding wall has broken or corroded away, however a crack has not yet developed. Bulges may contain localized cracking ("crblg") which has not yet developed into a circumferential or axial crack.

The term hydride ("hyd") is more general and refers to either a bulge or blister, but may also refer to a region that has not yet developed into a bulge. The last term "ec" refers to eddy-current indications, which may be hydrided areas of cladding which are not sufficiently visible as a bulge or hydride. The eddy-current probe consists of encircling coils through which the fuel rod (cladding) passes. Disturbances in the continuity of the material, imperfections or flaws, cracks and material changes, such as hydrides are registered by virtue of their effect on the eddy-current probe's electronic signal. Hydrides and eddy-current indications are considered minor forms of secondary degradation.

## 2.3 Description of the Fuel Operation

Utilities were surveyed with regard to the operating condition of the failed fuel. The general core operating details were available, however detailed fuel rod (or even assembly) power histories have proven difficult to obtain. In most cases, the beginning and end of cycle dates are readily available from the utilities or published data. For many cases, the dates of failure (and suppression when applied) are available. For several cycles where multiple failures occurred, or where the background "tramp" activity is high, it has proven very difficult to discern when the individual failures occurred. In at least two cases in which debris is determined to be the primary cause of failure, the date of failure is uncertain because the first indication of failure appears to coincide with the onset of severe secondary degradation.

One factor that may effect degradation is the type of control blade drive and core operating strategy which influence the magnitude of power changes on the fuel. In European BWRs of the ABB and Siemens designs, the control blade drives have a fine motion screw mechanism that enables a smooth continuous motion of the control blade. In contrast, GE plants have a ratchet (or notch) drive system, and the control blades are moved in discrete steps (of 6 inches). It is believed that such operation can cause significant power ramps on the fuel, particularly those fuel rods closest to the control blade.

The control blade management strategy may also play a role in the degradation of a failed rod, especially if the assembly containing the failure resides in an active control cell. With the advent of barrier fuel, many GE BWR utilities adopted the so-called control cell core operation (CCC) as opposed to a conventional core operation. In CCC operation, the utility utilizes one group (A2 in a GE BWR) of control rods throughout a cycle. Periodically, part of the group is deeply inserted into the core while the remainder of the group is slightly inserted (shallow) into the core. Exchanges occur at intervals of approximately 1.5 to 2.8 GWD/MTU of core exposure. In contrast, a conventional core strategy involves most of the control blades (all four groups A1, A2, B1, B2 of a GE BWR). The fuel which has operated in the vicinity of or adjacent to a deeply inserted control blade experiences a significant power increase when that control blade is withdrawn. Such a power increase can promote the propagation of an axial crack in the cladding of a failed fuel rod.

The suspected PCI failures in barrier fuel (Unk-Mfg, PCI-2) are believed to have been caused by the operation of the fuel in the control cell. In the case of cladding flaws, the rapid rise in local power caused sufficient stress in the cladding to cause to flaw the propagate. In the case of missing pellet surface, of which two cases have been confirmed, the cladding stresses were sufficiently high to cause the cladding to fail, even without a pre-existing cladding flaw. Since 1996, utilities have been operating with greater restrictions on the power ascension rates of barrier fuel.

Most European BWRs, which have traditionally operated on annual cycles, operate with a so-called Monosequence strategy in which one group of control blades is gradually withdrawn during the cycle. This strategy, while similar to CCC, avoids exchanging deep and shallow control blades. It is possible that with Monosequence operation in conjunction with alloy-liner and non-liner cladding, the power changes are sufficiently mild such that secondary degradation such as axial splits does not develop.

Utilities provided some information on water chemistry. Most European plants operate with normal water chemistry, i.e. without hydrogen or zinc injection. In the US, the trend is quite different with most plants injecting hydrogen, zinc or both. Failures have therefore occurred under a variety of water chemistry conditions, however none of the failures have occurred in plants with noble metal injection, which has only been introduced since 1998. There is apparently no dependence of secondary degradation on water chemistry.

## 2.4 References

1. [1] Davies, J.H., et. Al., "Post Irradiation Evaluation of BWR Fuel from Hope Creek Reactor," EPRI TR-106348, Final Report, November 1996.

2. [2] "Failure Root Cause of PCI Suspect Rod from Kernkraftwerk Leibstadt (KKL) Reactor, EPRI TR-111065-P2, June 2000.

# 3
# TRENDS IN FAILED BWR FUEL DEGRADATION

## 3.1 Alloy-liner and Non-barrier vs. Barrier (Pure Zr-liner) fuel

In response to the development of long axial splits in early barrier (liner) fuel, vendors began to consider alloying the liner to reduce the oxidation (corrosion) in the event of a cladding breach. ABB introduced a Zr-Sn liner during the early 1990’s and it quickly became the standard for that vendor; there are several failures in this population. Siemens introduced Zr-Fe liner cladding (Zr with approximately 0.3 - 0.4 w/o Fe) during the mid-1990's, and so far there are no failures in this population. GE has only recently (since late 1997) introduced a Zr-Fe alloy-liner cladding (with approximately 0.1 w/o Fe), and only one failure is so far reported in fuel with this cladding. GE's alloy liner represents an increase over the previous liner cladding in which the liner contained up to 400 ppm Fe in the liner and which was heated-treated for greater resistance to degradation. All of these alloy-liner, degradation resistant claddings were developed as alternatives to the high purity sponge liner claddings (100-200 Fe) common during the mid-1980's to mid 1990's.

**Table 3-1**
**Distribution of Degree of Degradation According to Cladding Type**

<table>
<tr><th rowspan="4">Clad Design</th><th rowspan="4">Totals of Reported Sec. Deg. (1-4)</th><th colspan="11">Degradation Category</th><th rowspan="4">Details of Secondary Degradation Unavailable</th><th rowspan="4">Total in database</th></tr>
<tr><th>Minor</th><th>Moderate</th><th colspan="3">Major [1]</th><th colspan="3">Severe [1]</th><th colspan="3">Maj+Sev.</th></tr>
<tr><th rowspan="2">(1)</th><th rowspan="2">(2)</th><th colspan="3">(3)</th><th colspan="3">(4)</th><th colspan="3">(3+4)</th></tr>
<tr><th>cr</th><th>cf</th><th>cr+ cf</th><th>cr</th><th>cf</th><th>cr+ cf</th><th>cr</th><th>cf</th><th>cr+ cf</th></tr>
<tr><td rowspan="3">Barrier</td><td rowspan="2">64</td><td rowspan="2">4</td><td rowspan="2">17</td><td colspan="3">26</td><td colspan="3">17</td><td colspan="3">43</td><td rowspan="3">29 (31 %)</td><td rowspan="3">93</td></tr>
<tr><td>13</td><td>8</td><td>5</td><td>16</td><td>1</td><td>0</td><td>29</td><td>9</td><td>5</td></tr>
<tr><td>100 %</td><td>6%</td><td>26 %</td><td colspan="3">41%</td><td colspan="3">27 %</td><td colspan="3">68 %</td></tr>
<tr><td>Alloy-bar.</td><td>5<br>100 %</td><td>0</td><td>5<br>100 %</td><td colspan="3">0</td><td colspan="3">0</td><td colspan="3">0</td><td>8 (62 %)</td><td>13</td></tr>
<tr><td rowspan="3">Non-barrier</td><td rowspan="2">31</td><td rowspan="2">9</td><td rowspan="2">8</td><td colspan="3">10[2]</td><td colspan="3">4</td><td colspan="3">14</td><td rowspan="3">35 (53 %)</td><td rowspan="3">66</td></tr>
<tr><td>4</td><td>4</td><td>1</td><td>0</td><td>3</td><td>1</td><td>4</td><td>7</td><td>2</td></tr>
<tr><td>100 %</td><td>29 %</td><td>26 %</td><td colspan="3">32 %</td><td colspan="3">13 %</td><td colspan="3">45 %</td></tr>
<tr><td>Totals</td><td>100</td><td>13</td><td>30</td><td colspan="3">36</td><td colspan="3">21</td><td colspan="3">57</td><td>72</td><td>172</td></tr>
</table>

[1] cr = axial crack, cf = circumferential crack
[2] One of 10 non-barrier failures had a ruptured hole and not a crack

Table 3-1 summarizes the degree of degradation by cladding design: barrier (with high purity Zr-liner), alloy-barrier and non-barrier. The degradation is categorized as discussed in Section 2. In the case of the 64 barrier cases for which information on secondary degradation was available, approximately 68% of the cases had major or severe degradation, while 26% had moderate degradation and 6% had minor degradation. The high fraction of major and severe degradation is significant when one considers that many of the failures were operated with some form of power suppression. Of the 31 non-barrier cases for which information on secondary degradation was available, 45% were reported to have major or severe degradation, while 26% had moderate and 29% had minor degradation. In contrast, all five of the alloy-barrier failures have moderate degradation. The statistics for this population are somewhat skewed by the fact that the details of secondary degradation of a relatively large fraction of the alloy-liner failures have not been made available. It would be expected that the degradation resistance of alloy-barrier cladding should be comparable to that of non-barrier cladding, because the corrosion resistance of the alloy-liner, while much greater than that of a pure-Zr liner, is similar to that of Zr-2.

On fact that is most striking in Table 3-1 is the proportion of barrier failures (29 of 64 failures, or 45%) that have axial cracks, of which 16 are considered severe. In contrast, only 4 or 31 non-barrier failures have axial cracks, all of which were rated as major, but none developed into a severe axial crack (> 6 inches). The data indicate that the non-barrier failures had a propensity for circumferential fractures, but more resistant to axial crack propagation.

The database contains information on twelve failures in fuel with Zr-Sn liner cladding and only one failure in fuel with Zr-Fe liner cladding. Comparing the secondary degradation of failures in the population of Zr-Sn alloy-barrier failures with those of similar non-barrier fuel designs, one observes that for primary defects at the upper spacer elevations, the development of secondary hydriding and degradation of alloy-liner and non-liner claddings occurs at similar elevations. More detailed comparisons of specific failures are provided in Appendix A. Table A-1 provides such a comparison among failures of alloy-liner (Zr-Sn) and non-liner fuel of similar design. All of the failures in this population are caused by debris, and most of these (19 of 23) had debris fretting in the upper spacers (4-7).

With respect to the single Zr-Fe liner failure in the database, the primary failure was located at Spacer 4 (approximately 80 inches). The secondary hydriding evolved into bulges and cracked bulges just below the first grid at elevations of 16-20 inches. This location corresponds to those at which bulges and circumferential cracks developed in some of the Zr-Sn alloy-barrier fuel and similar non-barrier fuel, which had debris fretting at the upper grids as mentioned above. This case is discussed in brief in Appendix A and in more detail in Section 4.

The distribution of failures in the database according to lattice type and cladding design is provided in Table 3-2. More details on the individual failures are provided in Table B-1, in Appendix B. The majority of 8x8 fuel (51 of 62 failures, or 82%) has barrier cladding with a pure Zr liner, while in the 9x9 population, 41 of 62 failures (66%) have pure Zr liner. In the 8x8 barrier fuel, severe or major degradation occurred in 28 of the 51 (55%) cases, and 21 failures developed axial cracks, of which 11 axial cracks (52%) exceeded 6 inches and are considered severe. Two of these cracks are most likely due to propagation of the primary defect due to local power conditions. The remaining smaller axial cracks had lengths ranging from less than 1 inch to approximately 5 inches. It is possible that they too could have extended if not for power suppression, as was the case for most 8x8 barrier failures. Five failures developed long axial cracks (> 6 inches), while 7 failures developed short axial cracks. In the 9x9 barrier population, severe or major degradation occurred in 21 of 41 (51%) cases. A comparison of the degradation of non-barrier and barrier (pure Zr) for 9x9-9Q/-9QA is provided in Table A-2. Only one non-barrier failure (out of the 11 for which data were available) developed an axial crack and this crack was less than 6 inches.

**Table 3-2**
**Distribution of Degree of Degradation According to Lattice Type and Cladding Design**

<table>
<tr><th rowspan="4">Lattice</th><th rowspan="4">Clad type</th><th rowspan="4">Totals of Reported Sec. Deg. (1-4)</th><th colspan="11">Degradation Category</th><th rowspan="4">Secondary Degradation Unavailable</th><th rowspan="4">Total in database</th></tr>
<tr><th>Minor</th><th>Moderate</th><th colspan="3">Major</th><th colspan="3">Severe</th><th colspan="3">Maj+Sev.</th></tr>
<tr><th rowspan="2">(1)</th><th rowspan="2">(2)</th><th colspan="3">(3)</th><th colspan="3">(4)</th><th colspan="3">(3+4)</th></tr>
<tr><th>cr</th><th>cf</th><th>cr+ cf</th><th>cr</th><th>cf</th><th>cr+ cf</th><th>cr</th><th>cf</th><th>cr+ cf</th></tr>
<tr><td rowspan="5">8x8</td><td rowspan="2">Bar.</td><td rowspan="2">43</td><td rowspan="2">2</td><td rowspan="2">13</td><td colspan="3">18</td><td colspan="3">10</td><td colspan="3">28</td><td rowspan="2">8</td><td rowspan="2">51</td></tr>
<tr><td>7</td><td>7</td><td>4</td><td>10</td><td>0</td><td>0</td><td></td><td></td><td></td></tr>
<tr><td>Alloy-bar.</td><td>1</td><td>0</td><td>1</td><td colspan="3">0</td><td colspan="3">0</td><td colspan="3">0</td><td>0</td><td>1</td></tr>
<tr><td>Non-bar.</td><td>4</td><td>2</td><td>1</td><td colspan="3">0</td><td colspan="3">1 cr+cf</td><td colspan="3">1 cr+cf</td><td>6</td><td>10</td></tr>
<tr><td>Sub-total</td><td>48</td><td>4</td><td>15</td><td colspan="3">18</td><td colspan="3">11</td><td colspan="3">29</td><td>14</td><td>62</td></tr>
<tr><td colspan="16"></td></tr>
<tr><td rowspan="6">9x9</td><td rowspan="2">Bar.</td><td rowspan="2">20</td><td rowspan="2">2</td><td rowspan="2">4</td><td colspan="3">7</td><td colspan="3">7</td><td colspan="3">14</td><td rowspan="2">21</td><td rowspan="2">41</td></tr>
<tr><td>1</td><td>5</td><td>1</td><td>6</td><td>1</td><td>0</td><td>7</td><td>6</td><td>1</td></tr>
<tr><td>Alloy-bar.</td><td>1</td><td>0</td><td>1</td><td colspan="3">0</td><td colspan="3">0</td><td colspan="3">0</td><td>0</td><td>1</td></tr>
<tr><td rowspan="2">Non-bar.</td><td rowspan="2">11</td><td rowspan="2">5</td><td rowspan="2">2</td><td colspan="3">4 [1]</td><td colspan="3" rowspan="2">0</td><td colspan="3">4</td><td rowspan="2">9</td><td rowspan="2">20</td></tr>
<tr><td>1</td><td>1</td><td>1</td><td>1</td><td>1</td><td>1</td></tr>
<tr><td>Sub-total</td><td>32</td><td>7</td><td>7</td><td colspan="3">11</td><td colspan="3">7</td><td colspan="3">18</td><td>30</td><td>62</td></tr>
<tr><td colspan="16"></td></tr>
<tr><td rowspan="4">10x10</td><td>Bar.</td><td>1</td><td>0</td><td>0</td><td colspan="3">1 cr</td><td colspan="3">0</td><td colspan="3">1 cr</td><td>0</td><td>1</td></tr>
<tr><td>Alloy-bar.</td><td>3</td><td>0</td><td>3</td><td colspan="3">0</td><td colspan="3">0</td><td colspan="3">0</td><td>8</td><td>11</td></tr>
<tr><td>Non-bar.</td><td>16</td><td>2</td><td>5</td><td colspan="3">3 cr + 3 cf</td><td colspan="3">3 cf</td><td colspan="3">3 cr + 6 cf</td><td>20</td><td>36</td></tr>
<tr><td>Sub-total</td><td>20</td><td>2</td><td>8</td><td colspan="3">7</td><td colspan="3">3</td><td colspan="3">10</td><td>28</td><td>48</td></tr>
<tr><td colspan="16"></td></tr>
<tr><td colspan="2">Totals</td><td>100</td><td>13</td><td>30</td><td colspan="3">36</td><td colspan="3">21</td><td colspan="3">57</td><td>72</td><td>172</td></tr>
</table>

[1] One of 4 9x9 non-barrier failures has a hole, not a crack

Overall, for failures in pure Zr-liner fuel, a substantial fraction (6 of 19 Siemens liner fuel rods and 22 or 77 GE liner fuel rods) developed axial cracks, certainly if not suppressed, but in some cases even with power suppression. On the other hand, a majority of failures with pure-Zr barrier cladding did not develop long axial cracks, which further suggests that local power conditions are the critical factor with the operating time in the failed state playing a secondary role and being dependent on local power conditions.

One factor that complicates the comparison between alloy-liner and non-liner failures with pure-Zr liner failures (most of which have occurred in the US) is the fact the great majority of pure-Zr liner failures have been suppressed. This then allows the fuel to operate at lower linear powers for long periods of time, and this tends to obscure the evolution of secondary degradation.

## 3.2 Primary Failures Modes and Secondary Degradation Type in 9x9 and 10x10 fuel

During the late 1980's, BWR utilities, particularly those in Europe, began to adopt 9x9 or 10x10 fuel depending on the fuel supplier. During the mid-1990's, US utilities began introducing reloads of 9x9 fuel, and only recently have introduced reloads of 10x10 fuel. Consequently, since 1993, one observes fewer failures in 8x8 fuel as time progresses, while an increasing number of failures have occurred in 9x9 and 10x10 fuel.

In comparing the severity of degradation among the populations of 8x8, 9x9 and 10x10 fuel designs provided in Tables 3-2 and B-1, one observes that the great majority of the 8x8 fuel has high-purity Zr-barrier cladding, and that 28 of the 43 failures in this population have major or severe degradation. In the 9x9-barrier population, 14 of 20 failures (70%) have major or severe degradation. Finally, the 10x10-barrier population consists of only one failure, which suffered major degradation.

In the alloy-barrier fuel group, there is one 8x8, one 9x9 and three 10x10 fuel rods for which details of the secondary degradation were obtained. All of these failures experienced moderate degradation. The degradation of alloy-barrier fuel tended to be similar to that of non-barrier fuel of similar design and to some extent burnup. However, it should be emphasized that there are additionally 8 alloy-liner failures for which the details of degradation were not available, and some of these do have major degradation.

In the non-barrier fuel population, there are 4 8x8, 11 9x9 and 16 10x10 fuel rods for which details of secondary degradation were obtained. Of these 31 failures, 9 experienced minor degradation, 8 had moderate degradation, 10 suffered major degradation, and only 4 experienced severed degradation. The major and severe degradation consisted of circumferential cracks and localized massive hydriding.

Within the populations of S64 (8x8) and S96/100 (10x10), most of which are debris failures, the location and type of the secondary degradation is comparable. Both populations suffer from secondary hydriding and in some cases circumferential fractures at similar locations. Therefore, one may conclude that failure degradation is not directly dependent upon fuel rod design, but instead, additional variables play a role.

In comparing the degradation of the GE7, GE8, GE9 and GE10 (8x8 designs with pure Zr liner) with those of the GE11, GE13 (9x9) and GE12 (10x10) designs, one observes comparable locations and types of secondary degradation. In particular, the population of failures with the debris fretting at the top spacer (sp 7), one can observe similar locations of secondary degradation among the populations of GE9 and GE10 failures and the population of GE11 and GE13 failures. Again, this trend of similar degradation evolution among 8x8, 9x9 and 10x10 failures supports the fact that fuel rod design is not so significant as are other variables, such as local power and the axial power shape (and to some extent burnup) in determining where the secondary hydriding will occur.

## 3.3 Suppressed vs. Un-suppressed Fuel

In the US, power suppression testing is often used to identify the core location of the leaking fuel rod. Following the identification of the assembly location, the leaker power is suppressed by inserting control blades in the cell containing the assembly. This is the generally accepted practice for mitigating degradation in a majority of the fuel that still contains a pure Zr-sponge liner. In Europe, where the fuel is a mix of either alloy-liner fuel or non-barrier (9x9 and 10x10), power suppression of leaking fuel rods is infrequently performed, partly from the concern of exacerbating the failure with power changes. Even European plants with failures in pure Zr-sponge liner tend not to suppress.

As has already been indicated, local power and axial power distribution are most likely the key factors in determining location and severity of secondary degradation. Therefore, it could be reasonably concluded that suppressing the fuel rod power should mitigate the progression of secondary degradation. However, a review of the degradation of suppressed fuel indicates that reduced power does not necessarily prevent severe secondary degradation, and this fact may be related to power level of the fuel prior to suppression. Although insufficient information is currently available to quantify this trend, the case studies discussed in Section 4 do indicate some effect of local power and axial power distribution.

Interestingly, many of the failures in European plants were not suppressed, yet the degradation was not severe in the sense of long axial cracks in non-liner or alloy-liner fuel. Two factors that may contribute to this trend are:

- Annual cycles and smaller batch sizes of European plants, which require a lower control blade density than 18 or 24-month cycles in US plants.
- Fine motion control rod drives with which control blades can be withdrawn at full power, but with fine continuous motion (with screw drive), and at finer steps than the notched control blades.

Clearly, in the case of liner fuel with the pure Zr-liner, the fine motion control blades has no advantage as is evidenced by the long axial and spiral splits in the 9x9-9QA fuel in one plant. Obviously, local power levels and time of operation in the failed state are the critical factor in such degradation.

## 3.4 Low vs. high burnup fuel

Sorting the database by burnup, one observes that burnup alone is not an important factor in the progression of secondary degradation. Rather it is indirectly related by virtue of the location of the fuel in the core and the power (and power changes) of the fuel. Of course, burnup is related to power generation in the sense that the higher burnup fuel usually operates at lower power levels. On the other hand, more modern fuel has higher enrichments in order to achieve greater burnup levels, and consequently, fuel of moderate burnup can operate at relatively high powers. In addition, in GE plants using the CCC operating mode, fuel with moderate burnup has traditionally been placed in the control cells with the consequence that the fuel will experience significant power changes.

A review of the debris failures in the S96/S100 population (in Table A-1) with discharge burnups in the range of 10 to 29.7 GWD/MTU indicates that degradation is essentially independent of burnup. A review of the GE and Siemens populations confirms that degradation is largely independent of burnup, and therefore local power and the axial power distribution are perhaps the more significant factors.

## 3.5 Time of Operation of Failed Fuel

Tables 3-3 to 3-6 provides a summary of the failures for which the time of failure was identified thus allowing for an evaluation of the impact of the length of time operated in the failed state on secondary degradation. As with burnup, data shows no direct dependence of secondary degradation with respect to time spent operating with a primary defect. Severe degradation, e.g. axial splits have been observed in fuel that operated for less than 20 days as well as fuel that has operated up to 577 days. Therefore, other variables, such as local power and axial power shape are more significant than operating time alone.

## 3.6 Distance Between Primary Defect and Secondary Degradation

Table 3-7 shows the database selections for which the locations of the primary and secondary defects were provided. The data are listed according to the primary location (axial elevation) and then burnup. One observes that most of the primary failures are debris, since the cause and location of the primary site are more easily identified for this mode of primary defect. Figure 3-1 shows the dependence of the distance between the primary defect and secondary degradation on the axial elevation of the primary defect. This distance represents the gaseous diffusion length along the fuel-cladding gap required to develop the necessary conditions for secondary hydriding.

For primary defects at the bottom of the fuel rod, the secondary degradation is usually high on the rod, mostly above 120 inches, and often involving a hydrided upper endplug. Two cases with debris fretting at the first grid spacer elevation also have secondary degradation toward the top of the fuel rod.

For all other cases where the primary defect occurs in the middle (> 55 in) and upper regions of the fuel rod, secondary degradation tends to develop in the bottom portion of the fuel rod. Figure 3-1 shows that secondary defects begin to form at least 35 inches away from the primary defect. As the location of the primary defect moves up the rod, the distance between the primary defect and secondary degradation expands, depending on the power level, axial power distribution and burnup. A minimum distance of 35 inches is shown in the data and appears to be independent of the axial elevation of the primary defect. The data highlighted in Figure 3-1 demonstrate that the predominance of a bottom-peaked power shape causes the secondary degradation to develop in the bottom portion of the rod for all situations of primary defects, except those at the extreme bottom of the rod. These results further support the conclusion that power level and power distribution are key factors in the development of secondary hydriding and the progression of secondary degradation.

Figure 3-2 shows the relationship between the primary defect location and the location of the secondary defects. Each group of data on the abscissa does not necessarily represent defects on one rod, but rather represents the defect locations on several rods having the same location of the primary defect. Referring to Figure 3-2, one observes that when the primary defect is in the upper portion of the fuel rod, the secondary degradation tends to occur toward the bottom of the fuel rod, and typically very near where the maximum local power in the rod is achieved. This is most likely why debris failures (or any failure) in the upper part of the fuel rod lead to long axial splits in barrier fuel, and localized circumferential fractures in non-barrier fuel.

**Table 3-3**
**Comparison of degradation of ABB failed fuel as a function of time in the failed state**

| Assembly Id. | Fuel Rod Position | Cause of Failure | Fuel Design | Burnup at Discharge (GWD/MTU) | Days in Failed State | Location of Primary Defect (inch) | Degree of Degradation | Location of Secondary Defect(s)* - (inch) |
|---|---|---|---|---|---|---|---|---|
| 21253 | F2 / J5 | Debris | S100 | 29.7 | 7 | 92 | major | 2 in. below sp 1 (crack) |
| 20790 | C7 / B6 | Debris | S64 | 14.5 | 14 | 111.7 | severe | cf (hyd) 11, cr 11-14.6 |
| 18834 | C2 / G6 | Debris | S64 | 19.2 | 29 | 110.2 | moderate | 17.7 |
| ABA010 | J1 / K10<br>F4 / G5 | Unk | S96 | 44.0 | 54 | n/a | n/a | n/a |
| 20681 | J10 / A1 | Debris | S100 | 32.3 | 78 | n/a | n/a | n/a |
| 21038 | I5 / F2 | Debris | S100 | 25.3 | | 134.3 | moderate | 41.3 |
| 19502 | H2/ J3, H3,<br>I2/ J2,<br>I3/ H2 | Debris | S100 | 22.8 | 83 | 0.0 | n/a | No severe hydriding |
| 23014 | B10 / A9 | Debris | S96 | 22.7 | 159 | 103.1 | moderate | 36.7 |
| ADB073 | A4 / G10 | Debris | S96 | 11.5 | 183 | 108 | severe | cf 25 |
| 21007 | D2 / J7 | Debris | S100 | 28.7 | 191 | 133.5 | moderate | 36.7 |
| 21965 | E2 / J6 | Debris | S96 | 23.2 | n/a | 118.1 | moderate | 43.3 |
| 18701 | G4 / E2 | Debris | S64AL | 33.3 | 197 | 132.7 | moderate | 19.7 |
| ACB116 | D5 / F7 | Debris | S96 | 19.1 | 245 | 108 | severe | cf 24 |
| 17790 | G3 / H4 | Debris | S100 | 24.3 | 278 | 87.8 | n/a | n/a |
| AFB129 | D7 | Debris | S96+/L | 12.0 | 301 | 108 | moderate | blg 25, crblg 4 |
| ABA010 | C8 | Debris | S96 | 10.5 | 318 | 92 | moderate | blgs below Sp 1 |
| AAA045 | B2 / J9 | Debris | S96 | 47.7 | 322 | 123 | minor | hyd 68-70 (Sp 3) |
| 17684 | G6 / E4 | Debris | S100 | 32.3 | 367 | n/a | n/a | n/a |

* Description of secondary defects
cr =crack, cf = circ frac, blg = bulge, crblg = cracked bulge, bls = blister, hyd = hydride, ec = eddy-current indication
n/a = not available

**Table 3-4**
**Comparison of degradation of GE failed fuel as a function of time in the failed state**

| Assembly Id. | Fuel Rod Position | Cause of Failure | Fuel Design | Burnup at Discharge (GWD/MTU) | Days Failed | Days Supp | Location of Primary Defect (inch) | Degree of Degradation | Location of Secondary Defect(s) - (inch) |
|---|---|---|---|---|---|---|---|---|---|
| YJ2802 | C5 | Debris | GE11B | 23.1 | 13 | 7 | 140 | moderate | crblg at 77 |
| YJB787 | A6 | Unk | GE10 | 18.8 | 16 | 0 | Unk | severe | cr 31-40, cr 40-115 |
| YJ8371 | G2 | Debris | GE8B | 1.2 | 19 | 0 | 140 | major | cf 21 |
| LYX042 | C6 | Debris | GE9B | 17.4 | 20 | 0 | 79 | severe | cr 19-28, cr 31-38, bls 16-50 |
| LYT305 | B7 | Mfg-Unk | GE7B | 30.7 | 20 | n/a | Unk | moderate | blg 8; blg 42-47; hyd 159 (UEP) |
| CAC158 | H4 | Mfg | GE9B | 20.1 | 25 | 12 | ?85.8 | moderate | 25.9,28.7,31.5 36 |
| HGE322 | Not Insp | CILC-II | GE11 | 17.0 | 41 | 35 | Not Insp | n/a | n/a |
| HGE340 | B2 | CILC-II | GE11 | 17.0 | 50 | 35 | 45 | n/a | n/a |
| YJ9760 | H7 | Debris | GE9B | 2.8 | 62 | 56 | 140 | major | cf 26, cf 28 |
| YJB806 | B5 | Debris | GE10 | 26.5 | 64 | 58 | 140 | major | cr 70-74 |
| YJD636 | H3 | Debris | GE9B | 14.0 | 66 | n/a | 142 | major | cf 159 (UEP), cf (sp1-sp2) |
| HGE337 | Not Insp | CILC-II | GE11 | 17.0 | 68 | 63 | Not Insp | n/a | n/a |
| YJD180 | E7 | Debris | GE13 | 28.3 | 69 | 54 | 132 | major | cr 70-73 |
| HGE339 | B2 | CILC-II | GE11 | 17.0 | 71 | 63 | 45-50 | n/a | n/a |
| YJ5168 | E1 | Unk - PCI? | GE9B | 33.26 | 74 | 0 | 55 | minor | hyd 19 |
| YJ8327 | A3 | PCI? | GE10 | 13.0 | 83 | 80 | Unk-22? | major | cr/cf 21-23.5 |
| YJ7372 | F1 | Debris | GE10 | 42.0 | 94 | 81 | 140 | moderate | blg 21, 66, 85, 92 |
| UB01GW | n/a | n/a | GE11B | 42.0 | 97 | n/a | n/a | n/a | n/a |
| LYL250 | A6 | Unk - PCI? | GE8B | 28.9 | 106 | 106 | Unk | severe | cr 13.4-16.1, 16.5-17.5, 29.9-36 |
| YJ2013 | G7 | Debris | GE10 | 26.4 | 109 | 96 | 140 | n/a | n/a |
| YJB856 | D1 | Debris | GE10 | ~26 | 115 | 105 | 120 | severe | cr 51-114 |
| LYL284 | A6 | Mfg- PCI? | GE8B | 28.9 | 119 | 107 | Unk | minor | ec 26-32 |
| HGE348 | H2 | CILC-II | GE11 | 17.0 | 142 | 86 | 33 | n/a | n/a |
| YJ7119 | B5 | Unk-Carryover | GE11B | 15.8 | 146 | 143 | Unk | severe | cf at 0 (LEP), cr 23-26, cr 15-16, blg 30 |
| YJE016 | J8 | Debris | GE11B | 30.0 | 149 | 137 | 0 | moderate | cr 141 |
| LYS488 | F8 | Debris | GE8B | 21.1 | 154 | 138 | 120 | moderate | blg 56 |
| HGE352 | A4 | CILC-II | GE11 | 17.0 | 170 | 153 | 50 | n/a | n/a |
| LYJ916 | H4 | Unk-Mfg | GE8B | 37.0 | 192 | 187 | Unk | moderate | blgs 28, 94, 96, 141, 146 |
| LYJ855 | D2 | Unk-Mfg | GE8B | 36.4 | 192 | 187 | Unk | major | Circ crack at 100-116, |

* Description of secondary defects
cr =crack, cf = circ frac, blg = bulge, crblg = cracked bulge, bls = blister, hyd = hydride, ec = eddy-current indication
n/a = not available

**Table 3-5**
**Comparison of degradation of GE failed fuel as a function of time in the failed state**

| Assembly Id. | Fuel Rod Position | Cause of Failure | Fuel Design | Burnup at Discharge (GWD/MTU) | Days Failed | Days Supp | Location of Primary Defect (inch) | Degree of Degradation | Location of Secondary Defect(s) - (inch) |
|---|---|---|---|---|---|---|---|---|---|
| LYJ855 | H4 | Unk-Mfg | GE8B | 36.4 | 192 | 187 | Unk | moderate | blgs 28, 30, 32 |
| LYJ855 | E8 | Unk-Mfg | GE8B | 36.4 | 192 | 187 | Unk | moderate | blgs 7, 11, 18,83, 85-100 |
| LYJ855 | F8 | Unk-Mfg | GE8B | 36.4 | 192 | 187 | Unk | major | crblgs at 121, 122; UEP blg, circ. crack |
| LYJ855 | G8 | Unk-Mfg | GE8B | 36.4 | 192 | 187 | Unk | moderate | blgs at 39, 59, 63,64,65, 118; crblg at 150 |
| HGE351 | F1 | CILC-II | GE11 | 17.0 | 198 | 190 | 52.5 | n/a | n/a |
| HGE351 | E1 | CILC-II | GE11 | 17.0 | 198 | 190 | 52.5 | n/a | n/a |
| HGE351 | A4 | CILC-II | GE11 | 17.0 | 198 | 190 | 52.5 | n/a | n/a |
| YJK861 | J6 | Debris | GE12B | 15.0 | 205 | 193 | 82 | major | cr 23-24, crblg 20, blg 10, 11 |
| YJ2624 | G6 | Debris | GE11B | 20.4 | 210 | 147 | 140 | moderate | crblg at 21 |
| LYG035 | A4 | Possible PCI | GE8B-4W | 30.0 | 220 | 206 | Unk | moderate | blg 58; ec 6, 46,59 |
| YJ4932 | F6 | Unk | GE9B | 22.4 | 223 | 218 | Unk | major | cr 11-15 |
| IGE646 | J4 | Debris | GE11 | 7.2 | 231 | 182 | 80 | moderate | crblg 17, 18, 19; blg21, 23; hyd 24-28 |
| YJ5835 | A3 | Debris | GE9B | 21.7 | 250 | 232 | 140 | severe | cr 31-62, cr 62-112 |
| YJ2263 | C4 | Mfg-LEPW | GE8B | 11.2 | 257 | n/a | 0 | major | cf 159 |
| LYA354 | B4 | Debris | GE7B | 26.8 | 277 | n/a | 1 | n/a | n/a |
| LYA459 | C3 | Mfg- PCI? | GE7B | 26.8 | 307 | n/a | Unk | major | cr 30, cf 159 (UEP) |
| UB01HZ | n/a | n/a | GE11B | 39.2 | 307 | n/a | n/a | n/a | n/a |
| YJ1590 | G9 | Unk (Deb, mfg) | GE11B | 29.2 | 349 | 322 | n/a | severe | crblg 6, 35; blg 8, 37; cr 65, 67-121 (spiral); cf 76 |
| LYG021 | F1 | Mfg- PCI? | GE8B-4W | 28.1 | 368 | 358 | Unk | moderate | cr 137-138; crblg 3 |
| LYG037 | A6 | Mfg- PCI? | GE8B-4W | 27.9 | 368 | 358 | Unk | major | cr 140; ec 45, 43, 46, 140,142,144 |
| LYZ621 | G4 | Unk | GE9B | 36.8 | 373 | 366 | Unk | major | cr 51, cr 78-81; blg 139 |
| ND099 K | ?? | No insp yet | GE11T | 22 | 380 | | No insp yet | n/a | No insp yet |
| YJ8594 | D1 | Debris | GE10 | n/a | 396 | 379 | 120 | severe | Multiple cracks 10-130 |
| LYP571 | D1 | Mfg- PCI? | GE8B | 29.6 | 417 | 410 | Unk | major | cr 28-40, cf 159 (UEP) |
| LYX334 | n/a | No insp | GE10 | 21.1 | 443 | 424 | n/a | n/a | n/a |
| LYA232 | A4 | Mfg- PCI? | GE7B | 24.4 | 520 | n/a | Unk | severe | cr 30-34, cr 70-110 |
| YJD643 | B3 | Unk - Debris? | GE9B | n/a | 577 | 201 | Unk | major | cr/cf 25-30 |
| LYL294 | B2 | Unk-Debris | GE8B | 29.0 | 667 | 497 | Unk | major | blg 159, cf 159 (UEP) |

* Description of secondary defects
cr =crack, cf = circ frac, blg = bulge, crblg = cracked bulge, bls = blister, hyd = hydride, ec = eddy-current indication
n/a = not available

**Table 3-6**
**Comparison of degradation of Siemens failed fuel as a function of time in the failed state**

| Assembly Id. | Fuel Rod Position | Cause of Failure | Fuel Design | Burnup at Discharge (GWD/MTU) | Days Failed | Location of Primary Defect (inch) | Degree of Degradation | Location of Secondary Defect(s) - (inch) |
|---|---|---|---|---|---|---|---|---|
| 0769 | C1 | PCI | 9-1 | 29.2 | 32 | n/a | n/a | n/a |
| 0519 | n/a | Unk, PCI? | 9-1 | 30.9 | 36 | n/a | n/a | n/a |
| 0668 | A5 | PCI | 9-1 | 30.2 | 89 | n/a | n/a | n/a |
| 0823 | n/a | Unk, PCI? | 9-1 | 34.8 | 167 | n/a | n/a | n/a |
| JB 039 K | K9 | Debris | 9-9QA | 11.8 | 186 | 98.5 | severe | cr 23.6 - 61; bulges 11.4, 13.8, 15.5, 18.1 |
| JB 075 K | G1 | Debris | 9-9QA | 8.2 | 255 | 80 | severe | spiral cr 19.7-26, cr 26-30 |
| 0578 | C1 | Unk, PCI? | 9-1 | 30.4 | 345 | n/a | n/a | n/a |
| | | | | | | | | |
| KAA119 | K3 | Debris | 9-2 | 27.0 | 10 | n/a | n/a | No significant degradation |
| XNC-827 | B5 | Unk-debris, PCI | 8x8 | 26.3 | 26 | 60 | minor | No significant degradation |
| AND018 | A2 | Unk-debris, PCI | 9-5 | 14.7 | 83 | 130-133 | minor | No significant degradation |
| AND122 | A5 | Unk-debris, PCI | 9-5 | 15.2 | 144 | 81-83 | minor | No significant degradation |
| AND043 | B4 | Debris | 9-5 | 22.1 | 315 | 140 | minor | No significant degradation |
| SPF767 or 768 | n/a | No exam | 9-5 | ~26 | 407 | n/a | n/a | No apparent significant degradation |
| KS2581 | F3 | Unk | 8-2 | ~30 | 415 | n/a | minor | No significant degradation |
| X24885 | C9 | Unk | 9-2 | 23.2 | 459 | unk | minor | hyd 25,70,135 |
| A3W034 | H2 | Unk | 9x9-2L | 14.0 | <633 | unk | severe | cf 12 |

* Description of secondary defects
cr =crack, cf = circ frac, blg = bulge, crblg = cracked bulge, bls = blister, hyd = hydride, ec = eddy-current indication
n/a = not available

**Table 3-7**
**Trends in the Secondary Degradation Location as a Function of Primary Location**

| Assembly ID | Rod Location ABB/GE | Cause of Failure | Fuel Design | Disch. Burnup GWD/ MTU | Loc. of Primary Defect (inch) | Location of Degradation (inch) cr =crack, cf = circ frac blg = bulge, crblg = cracked bulge bls = blister, hyd = hydride ec = eddy-current indication | Approx. Distance Primary to Secondary |
|---|---|---|---|---|---|---|---|
| KD005K | A4 | Mfg-LEPW | GE11 | 9.0 | 0 | cr 144 (small) above Sp 7 | 144 |
| YJ2263 | C4 | Mfg-LEPW | GE8B | 11.2 | 0 | cf 159 | 159 |
| YJE016 | J8 | Debris | GE11B | 30.0 | 0 | cr 141 | 141 |
| HA 082 K | D7 | Debris | 9-9Q L | 33.0 | 0 | cr 126-127.5 | 126 |
| HA 067 K | C4 | Debris | 9-9Q L | 35.9 | 0 | EC (inside) signals 137-149, blg 159 | 143 |
| HA 057 K | G7 | Debris | 9-9Q L | 36.0 | 0 | cf 145 | 145 |
| HA 095 K | G4 | Debris | 9-9Q L | 41.9 | 0 | EC (inside) signals 126 above LEP | 126 |
| JM064 | E2 | Debris | 8-2L | 27.9 | 20.5 | cf at UEP | ~140 |
| KU0679 | B5 | Debris | 9-9QA nL | 35.7 | 20 | blg below sp 6 | ~100-120 |
| YJ5168 | E1 | Unk - PCI? | GE9B | 33.26 | 55 | hyd 19 | 36 |
| ND098K | E8 | Debris | GE11T | 7.0 | 80 | cr 21.7 | 58 |
| IGE646 | J4 | Debris | GE11 | 7.2 | 80 | crblg 17, 18, 19; blg21, 23; hyd 24-28 | 50-63 |
| JB 075 K | G1 | Debris | 9-9QA L | 8.2 | 80 | spiral cr 19.7-26, cr 26-30 | 50-60 |
| YJK861 | J6 | Debris | GE12B | 15.0 | 82 | cr 23-24, crblg 20, blg 10, 11 | 55-70 |
| LYX042 | C6 | Debris | GE9B | 17.4 | 79 | cr 19-28, cr 31-38, bls 16-50 | 30-50 |
| KU0863 | A3 | Debris | 9-9QA nL | 19.4 | 80 | axial crack between sp 1 and 2 | 40-60 |
| CAC158 | H4 | Mfg | GE9B | 20.1 | 85.8 | 25.9,28.7,31.5, 36 | 50-60 |
| 21253 | F2 / J5 | Debris | S100 | 29.7 | 88 | 2 in. below spacer 1 (crack) @ 19 | 69 |
| ABA010 | C8 | Debris | S96 | 10.5 | 92 | blgs below sp 1 (21) | >70 |
| KLG072 | B4 | Mfg | GE10 | 27.2 | 94 | X-mark 94-95; blg 16 | 79 |
| JB 039 K | K9 | Debris | 9-9QA L | 11.8 | 98.5 | cr 23.6 - 61; bulges 11.4, 13.8, 15.5, 18.1 | 37-65, >80 |
| KU0787 | B7 | Debris | 9-9QA nL | 19.6 | 100 | small cf below sp 1 (21) | >80 |
| 23014 | B10 / A9 | Debris | S96 | 22.7 | 103.1 | 36.7 | 66.3 |
| KLG055 | F3 | Mfg | GE10 | 27.0 | 100 | cr 86-120 (propagating primary); bl 7 | 93 |
| ACA026 | A3 / H10 | Debris | S96 | 8.8 | 108 | cf 29 | 79 |
| ADB073 | A4 / G10 | Debris | S96 | 11.5 | 108 | cf 25 | 83 |
| AFB129 | D7 | Debris | S96+/L | 12.0 | 108 | blg 25, crblg 4 | 83 |
| 20790 | C7 / B6 | Debris | S64 | 14.5 | 111.7 | cf (hyd) 11, cr 11-14.6 | 97-101 |
| ACB116 | D5 / F7 | Debris | S96 | 19.1 | 108 | cf 24 | 84 |
| 18834 | C2 / G6 | Debris | S64 | 19.2 | 110.2 | 17.7 | 92.3 |
| AEC092 | J6 / E1 | Debris | S96 | 24.8 | 108 | cf (sp 1/sp2) | 67-87 |
| ACA031 | J4 / G1 | Debris | S96 | 9.2 | 123 | cf 32 | 91 |
| AFB072 | H4 / G3 | Debris | S96+/L | 12.0 | 123 | blg (sp 1/sp2) | 80-102 |
| LYX155 | E3 | Debris | GE9B | 17.5 | 121.5 | cr 30-33 | 90 |
| LYS488 | F8 | Debris | GE8B | 21.1 | 120 | blg 56 | 64 |
| 21965 | E2 / J6 | Debris | S96 | 23.2 | 118.1 | 43.3 | 75 |
| YJB856 | D1 | Debris | GE10 | ~26 | 120 | cr 51-114 | 6-70 |
| KU0948 | A9 | Debris | 9-9QA nL | 29.3 | 120 | blgs, hole below sp 1 | >100 |
| YJ8594 | D1 | Debris | GE10 | ~>30 | 120 | Multiple cracks 10-130 | 0-110 |
| AAA045 | B2 / J9 | Debris | S96 | 47.7 | 123 | hyd 68-70 (Sp 3) | 54 |
| 21145 | E8 / C6 | Debris | S100 | 10.1 | 133 | cf (LEP and sp 1) | >112 |
| 20490 | G4 | Debris | S100 | 12.5 | 133 | 15.4 above LEP | 118 |
| 18945 | J9 / B1 | Debris | S100 | 23.7 | 133 | 6 in. crack below sp 1 | >112 |
| 21038 | I5 / F2 | Debris | S100 | 25.3 | 134.3 | 41.3 | 93 |
| YJD180 | E7 | Debris | GE13 | 28.3 | 132 | cr 70-73 | 60 |
| 21007 | D2 / J7 | Debris | S100 | 28.7 | 133.5 | 36.7 | 97 |
| 18701 | G4 / E2 | Debris | S64AL | 33.3 | 132.7 | 19.7 | 113 |
| YJ8371 | G2 | Debris | GE8B | 1.2 | 140 | cf 21 | 120 |
| YJ9760 | H7 | Debris | GE9B | 2.8 | 140 | cf 26, cf 28 | 112-114 |
| AFB080 | I3 /H2 | Debris | S96+/L | 12.0 | 139 | blg 45 (sp 2), crblg (below Sp 1) | 94 |
| YJD636 | H3 | Debris | GE9B | 14.0 | 142 | cf 159 (UEP), cf (sp1-sp2) | 112 |
| YJ2624 | G6 | Debris | GE11B | 20.4 | 140 | crblg at 21 | 119 |
| YJ5835 | A3 | Debris | GE9B | 21.7 | 140 | cr 31-62, cr 62-112 | 69 |
| YJ2802 | C5 | Debris | GE11B | 23.1 | 140 | crblg at 77 | 63 |
| YJB806 | B5 | Debris | GE10 | 26.5 | 140 | cr 70-74 | 68 |
| YJ7372 | F1 | Debris | GE10 | 42.0 | 140 | blg 21, 66, 85, 92 | 48-119 |

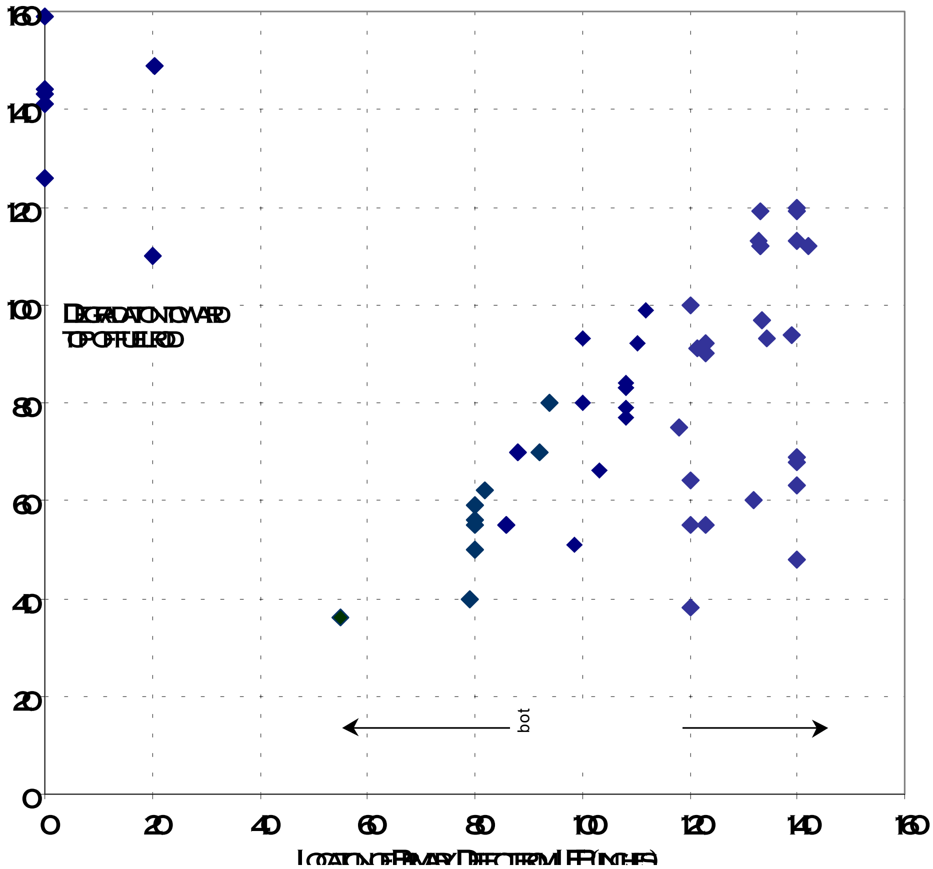


**Figure 3-1**
**Distance to Secondary Defects as a Function of the Location of the Primary Defect**

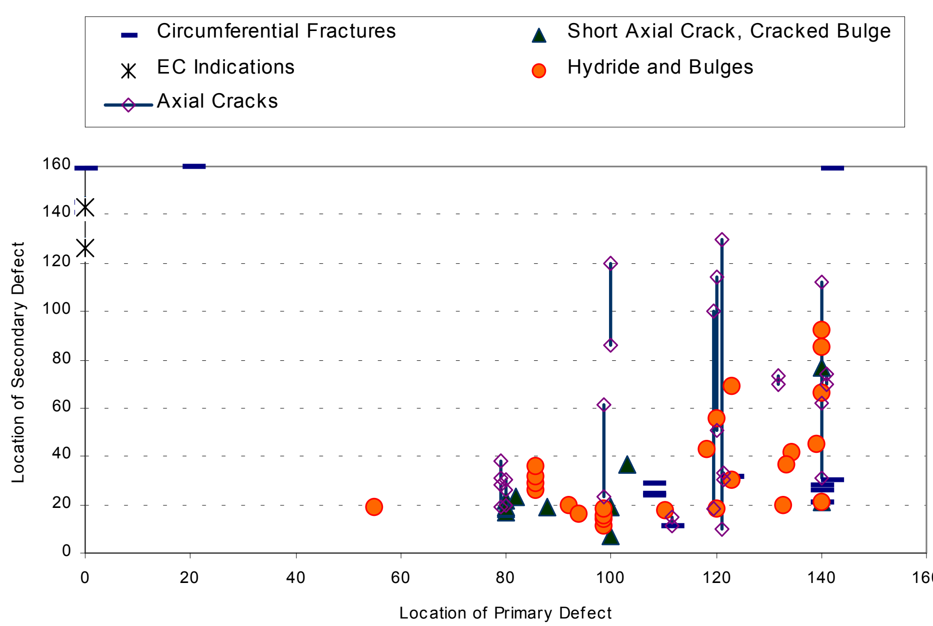


**Figure 3-2**
**Location of Secondary Degradation as a Function of the Location of the Primary Defect**

# 4 CASE STUDIES

Four sets of cases for which axial power profiles were obtained are discussed. For three sets, the secondary hydriding and degradation occurs at the location of peak linear power at the time of failure, or shortly thereafter. In the fourth case, the axial power profile is relatively uniform, i.e. without a substantial power peak, but the secondary hydriding and degradation occurred at the point just beyond the peak power location. The fifth set provides a summary of three barrier failures (1 8x8, 1 9x9 and 1 10x10) in one plant.

**Limerick-1** - Cycle 8 began on May 22, 1998 with a steady-state Σ6 off-gas activity of approximately 1600 µCi/sec. The off-gas activity increased to approximately 4800 µCi/sec on September 30, 1998 before settling to a level around 3500 µCi/sec. During the period, October 8-12, the utility reduced power to 61% power for flux tilting. The sum of 6 had achieved a peak level of 4200 µCi/sec before the flux tilting. There was some difficulty with the sensitivity of the off-gas activity monitoring during the flux tilt campaign. Due to some uncertainty in the precise core location of the failure, the utility elected to insert 6 control rods in order to suppress the failure.

As expected, given another 18 months in the current Cycle 8 and indications of potential fuel degradation due to Np-239 in the core, PECO decided to implement a mid-cycle outage to remove the failure. The fuel had operated 65 days in the defected state during and with suppression for 58 days. During the mid-cycle outage, PECO identified one failed GE13 fuel assembly with a rod (E7) failed by debris. A debris-fretting hole was identified at spacer 7 (132 inches) and a secondary defect in the form of a short axial split had developed at an elevation of 70-73 inches. The location of the secondary defect is consistent with most other debris failures in which the primary failure occurs at an upper spacer, and the secondary degradation occurs at a remote location (in this case approximately 60 inches away).

The axial power shapes for this rod during Cycle 8 are provided in Figure 4-1. The short axial crack (70-73 inches) is located at the peak power location (node 12) at the time of failure (on September 26, 1998. The power level at the time of failure was approximately 7.2 kW/ft. Prior to the failure indication, the local power had been steadily increasing from a level of 6.67 kW/ft to the value of 7.2 kW/ft. Shortly after the failure, the power shifted away from node 12 to nodes 10 and 11. These events are significant, since it is possible that the fuel rod had failed before any indication in the plant monitoring equipment. Since the short crack occurred at the peak power location and did not propagate, it is possible that the power change after the rod failed was not significant for crack propagation. This may indicate that the failure initiated a short time before September 26.

The fuel assembly was operating in the early part of its second cycle, which means that the fuel was fabricated sometime in the later part of 1995, or possibly in 1Q 1996, and the cladding is a Process 6 design. The failure was similar to that of the failure in Cooper, Cy 17 in the sense that the first indication of failure most likely coincided with the onset of secondary degradation. It is possible that the debris was entrapped in the wear-hole, which prevented the escape of off-gas during operation.

**River Bend -** Cycle 9 began July 3, 1999 after a cycle in which multiple corrosion failures had occurred. Within two weeks a new failure occurred. The Σ6 off-gas activity was initially unsteady at approximately 6000 μCi/sec, but settled between 3000 and 4000 μCi/sec. The utility performed one flux tile during mid-Aug, but was unsuccessful in locating the failure. A second flux tilt was performed on September 4, 1999, approximately 50 days after the initiation of the failure.

At the end of the cycle, the utility identified one failed rod (J7) in a GE11 fuel assembly. The cladding was Process 7 (with a new Fe-enhanced liner). The primary defect was a debris fret at spacer 4, and the secondary degradation consisted of multiple hydride bulges at 17-23 inches. Some bulges at 17, 18 and 19 inches were cracked.

The failure operated for approximately 182 days with one control blade inserted for power suppression. The axial power shapes at time of failure, after suppression and at EOC are provided in Figure 4-2. Although it operated at a peak local power of 10.3 kW/ft for approximately 49 days, the secondary degradation consisted of bulges, some of which were cracked, but it did not evolve into a circumferential fracture. This is in contrast to the S96 and S100 failures (with both alloy-liner and non-liner cladding) of which many developed circumferential cracks.

The peak power location at time of failure coincides with the location of the significant hydriding - actually the hydriding occurred just beyond the peak power location. A possible explanation would be that at the peak power location, any remaining steam was converted (through the corrosion process) to hydrogen and thus the area of the fuel below the peak power location experienced a dry hydrogen (oxygen-starved) region, which is the requirement for severe hydriding.

**Ringhals 1** - Cycle 20 began November 22, 1997 and within 7 days the off-gas activity indicated a failure. At the time of the failure, the plant was operating at approximately 80% of full power. The plant reduced power to approximately 10-15% followed by an ascension to full power. After a few days of operating at full power, the plant went into an outage to remove the failed fuel on December 12, fourteen days after the failure was detected.

During the outage, the utility identified one failed fuel rod (C7 - equivalent to B6 in GE/Siemens lattice) in a SVEA-64 assembly. The primary cause of failure was a debris fret at spacer 5 at an elevation of 111.7 inches. Secondary degradation occurred, as expected, at a lower elevation (11 - 15 inches). At the 11-inch elevation, the fuel rod had suffered a guillotine fracture as the result of massive local hydriding. A short axial crack extended above the guillotine break from 11 inches to approximately 15 inches. Another shorter axial, which appeared to be the development of a spiral fracture, was located 45° azimuthally from the longer crack and extended only about 0.5 inches.

The axial power shapes for this rod are provided in Figure 4-3. This case is interesting considering the relatively flat power profile and the absence of significant power peaking. The massive hydriding and localized degradation occurred just beyond the peak power location, rather than at the peak power location. The severity of degradation that occurred is what one might expect for a failure in high purity Zr-liner cladding. Quite possibly, the significant changes in power contributed to the rapid degradation (14 days) process.

**KKL** - During Cycle 10A, the unit experienced multiple failures, which include 3 GE 8x8 barrier fuel assemblies and two ABB non-barrier (S96) assemblies. Immediately following the start-up of the unit there was an indication of failure, which the utility indicates may have failed in the previous cycle (or was an incipient failure that was carried over).

The first indication of failure (slight transient (spike) in the Xe-133 off-gas activity) that was eventually attributed to one of the SVEA-96 fuel elements occurred on October 14, 1993 (Day 38). A second indication, also a slight transient in the Xe-133 activity, occurred on November 21 (Day 78). Subsequently, there were two increases in the steady-state Xe-133 and Xe-135 off-gas activities, which were accompanied by increases in the steady-state I-131 and I-133 coolant activities, on December 6 (Day 91) and December 23 (Day 108) respectively. The increases in steady-state off-gas and coolant activities indicate the onset of secondary degradation, and it is believed that these events were the development of the circumferential fractures in the S96 fuel.

Assuming that the first degradation event (on Day 91) coincided with the first indication of failure (Day 38), then the development of the circumferential fracture required 53 days. The development of the second fracture then required 30 days based on failure at day 78 and an indication of degradation on Day 108.

The axial power shapes for the two failures, ACA026 A3 and ACA031 J4, are provided in Figures 4-4 and 4-5. Both fuel rods had similar axial power shapes and magnitudes of peak power at the same time, therefore it is difficult to determine which of the elements failed or degraded at which moment. Despite the fact that one rod had a debris failure at Spacer 6 and the other had a debris failure at Spacer 5, both rods developed circumferential fractures at similar elevations. This elevation coincided with the location of peak power during the period when the failures occurred and when they apparently degraded.

**Perry** - Cycle 7 began on October 23, 1997. Scrams occurred in December 1997 and on July 1 1998. The July 1 1998 scram also incurred a RCIC and HPCS injection to the reactor vessel. Perry performed flux tilting during the period of Sep 12-14, 1998 following an increase in off-gas on September 3. The off-gas was very low for this failure, with low Kr and short-lived Xe activities in the off-gas. A spike in Xe-133 indicated a possible second failure during late October. Perry flux-tilted again during the weekend of Nov 7-9 and power suppression was implemented. A third PST was performed in December 1998. The Cycle ended on March 27, 1999, with the reactor operating at 87.7% of full-rated power.

YJK861 Rod J6, GE12 Process 6 -

One defect was attributed to unidentified debris at the fifth spacer (approximately 120 inches). A 0.7-inch secondary hydride crack was also noted at an elevation of approximately 23 inches. This defect was detected on September 3, 1998, followed by power suppression with 2 control rods. In early December an increase in iodine (which had fallen back to beginning of cycle values) was noted, and a third control rod was inserted. The iodine activity then decreased. The utility believes that the formation of the secondary crack coincided with the iodine increase. The failure operated for a total of 205 days with 193 days with power suppression. The degradation consisted of a small crack at an elevation of 23 inches, a cracked bulge at 20 inches and two bulges at 10 and 11 inches.

YJE016 Rod J8, GE11 Process 6 -

One defect was attributed to debris at the lower tie plate (a 2-inch shard of stainless steel strip was sticking up through the lower tie plate). No detailed examination of the rod was performed since the cause of failure was easily established, but a small crack was noted at approximately 141 inches. This defect occurred in October 1998, and was suppressed by insertion of 2 control rods. The failure operated a total of 149 days of which 137 days were with power suppression.

YJ7372, Rod F1, GE10 Process 5 -

Debris fretting occurred at the top spacer (Sp 7). The defect was considered very tight and could only be confirmed by gas slowly bubbling out. Secondary degradation consisted of bulges at 21, 66, 85, 92 inches. Since the rod was a tie rod, it was not removed from the bundle. This defect was detected on December 21, 1998 and was suppressed by insertion of 1 control rod (since plant was nearing all rods out). The failure operated 94 days including 81 days with power suppression.

Among these three failures, one observes that the two failures (GE12 and GE11) with longer operating time in the failed state developed small cracks as compared to bulges in the GE10. Therefore burnup or time of operation in the failed state are not considered a singularly significant factors in degradation.

The details among these case studies offer some idea of the complexity of the degradation process. The one 8x8 non-barrier case severely degraded within 14 days. The (9x9) GE11 alloy-barrier and 10x10 (S96) non-barrier cases developed significant hydriding near the peak power location, but the GE11 alloy-barrier failure did not degrade by circumferential fracture, whereas the non-barrier 10x10 failures did. The local power level and power distribution appear to be significant factors in evolution of degradation in conjunction with the location of the primary defect. Detailed information from additional case studies is required in order to better understand (quantify) the combined effects of power, primary defect location, as well as burnup and time in the failed state.

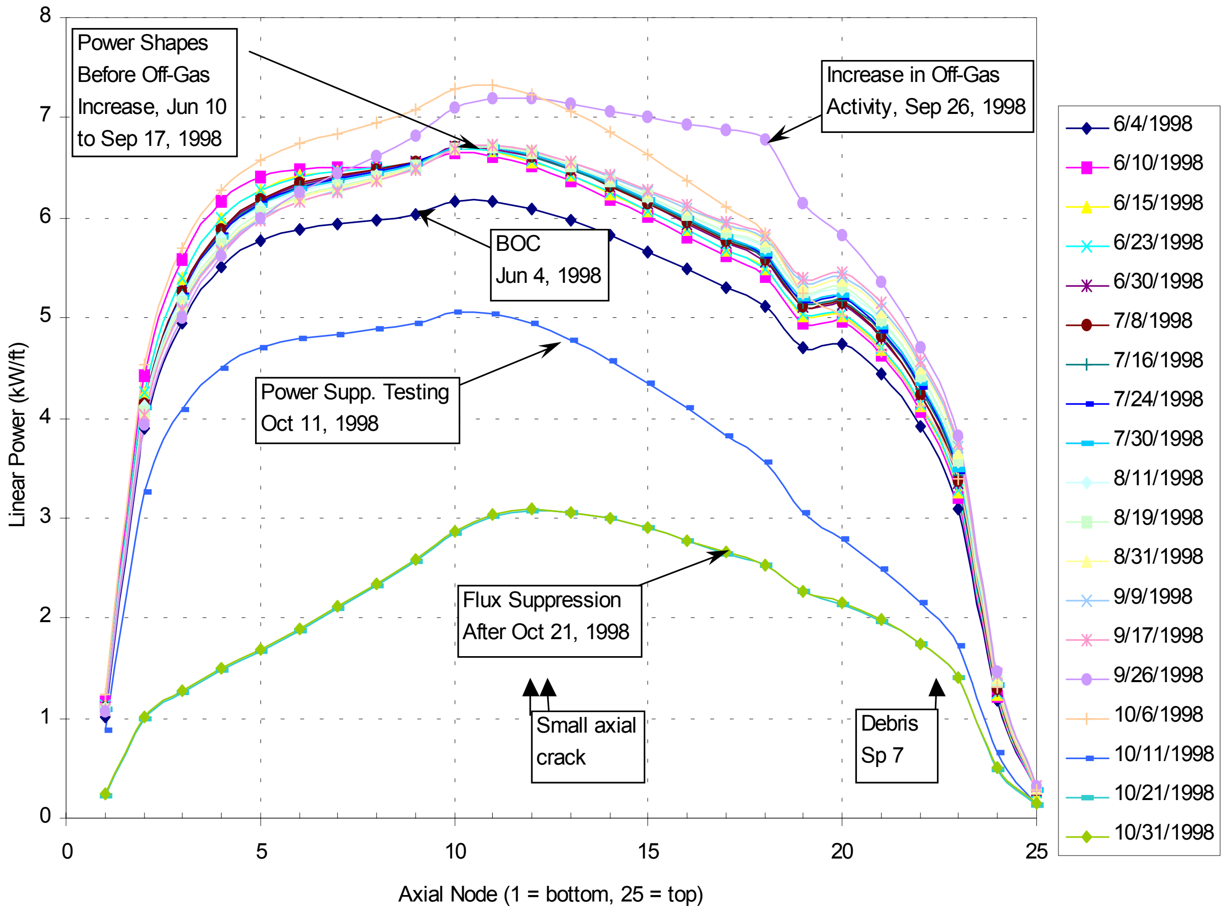


**Figure 4-1**
**Axial Power Profiles for YJD180 E1.**

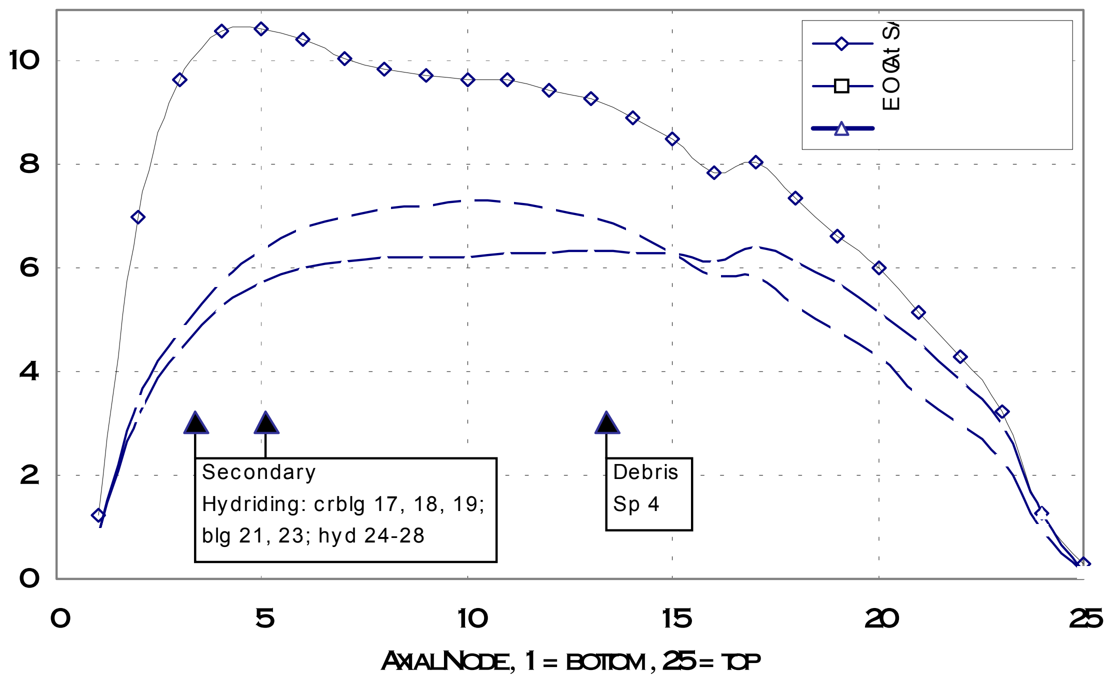


**Figure 4-2**
**Axial Power Profiles of IGE646 J4**

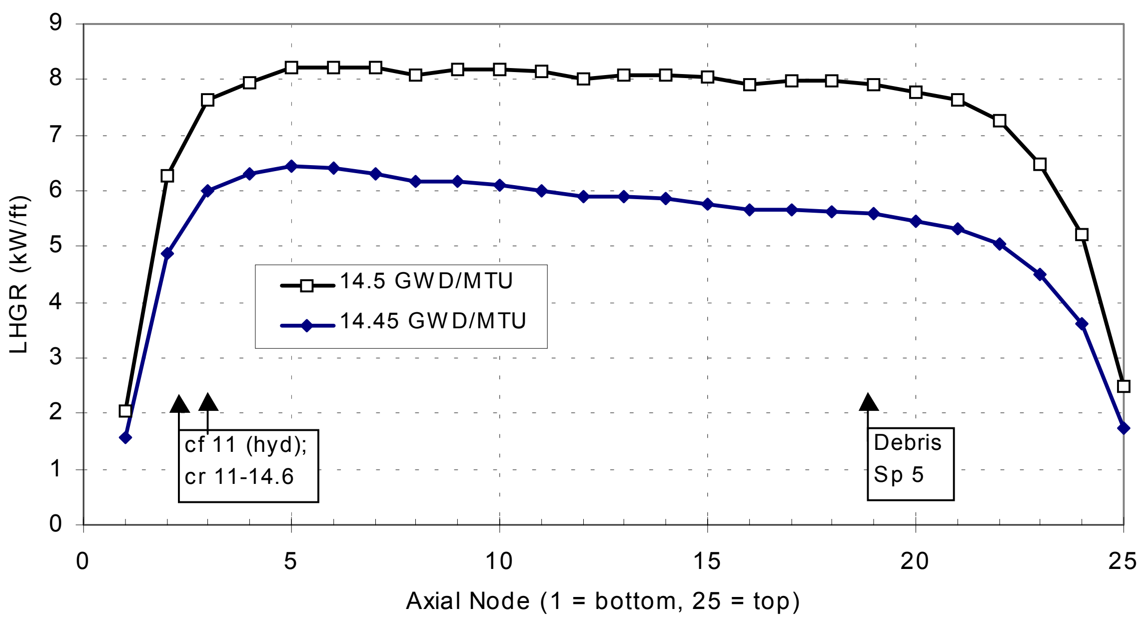


**Figure 4-3**
**Axial Power Profiles of 20790 C7 (B6) Prior to Mid-cycle Outage**

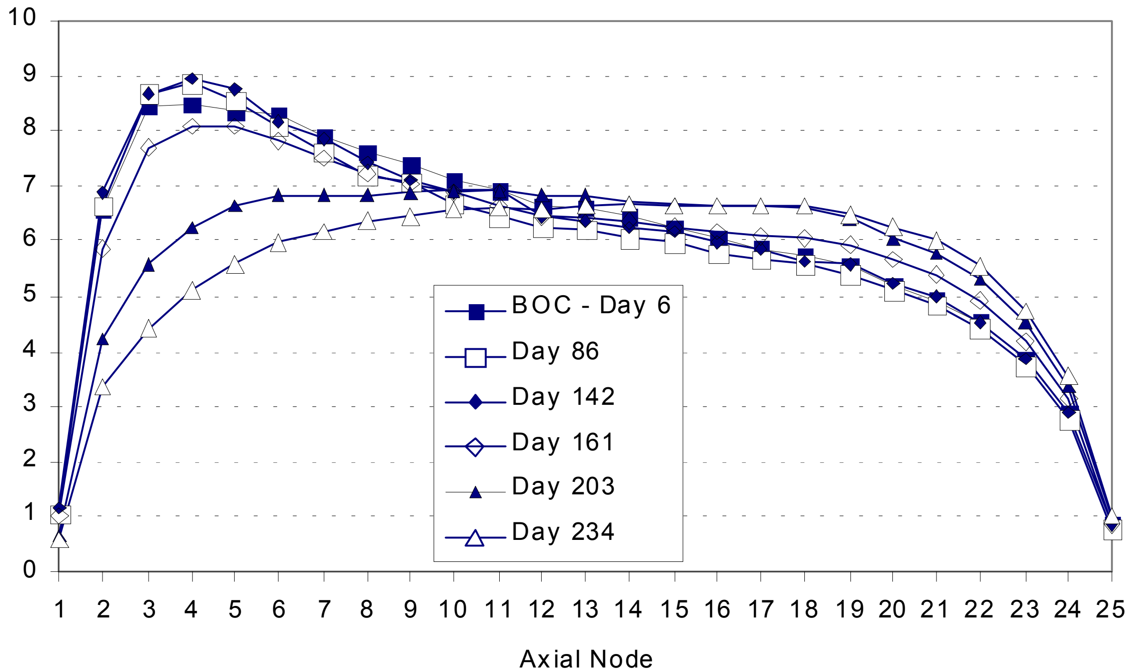


**Figure 4-4**
**Axial Power Profile of ACA026 A3.**

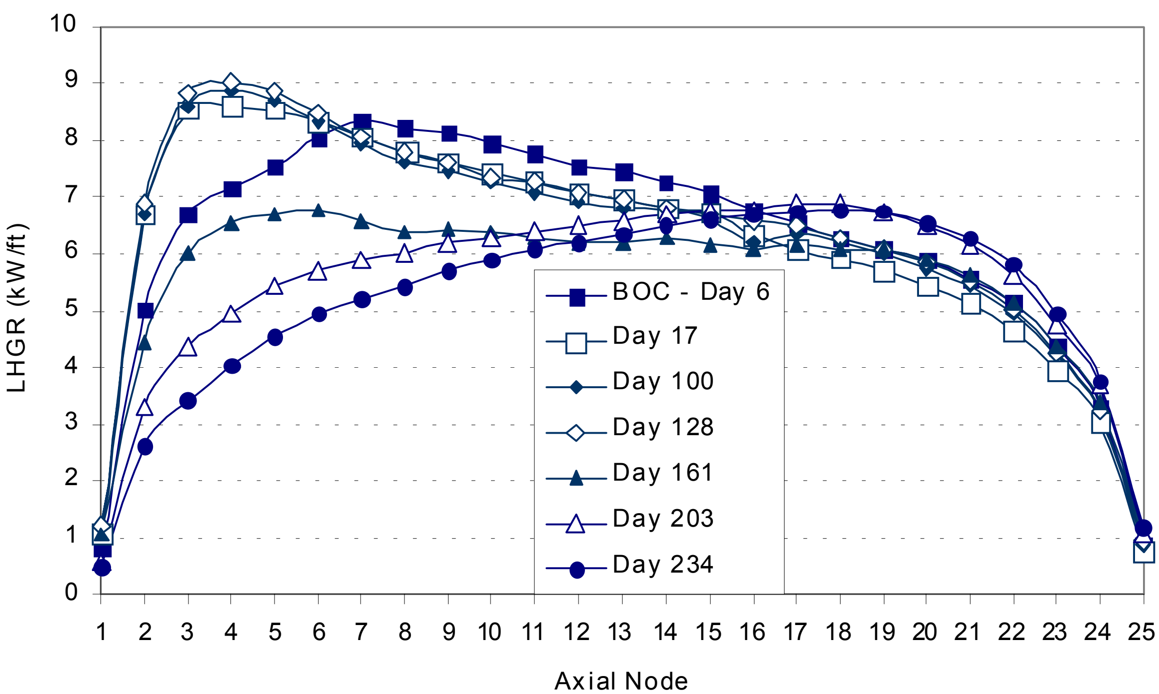


**Figure 4-5**
**Axial Power Profile of ACA031 J4**

# 5
# RESULTS AND CONCLUSIONS

An extensive database of BWR fuel failures has been developed. Data are provided for 172 cases, which have occurred in cycles concluding from 1993 (although 6 cases originated in 1992) to first quarter of 2000. The database includes many of the modern BWR fuel designs of the 9x9 and 10x10 lattices, and several cases of alloy-liner fuel.

Trend analyses were performed to evaluate the dependence of failure degradation with respect to:

- Cladding design: barrier (Pure Zr-liner), alloy-liner, and non-barrier
- Fuel design: 8x8, 9x9 and 10x10 fuel
- Power: Suppressed vs. non-suppressed (low and high power) fuel
- Low vs. high burnup fuel
- Time of operation with primary defect
- Distance Between Primary Defect and Secondary Degradation

It is observed that barrier fuel with a pure Zr-liner on the inner surface of the cladding have a propensity to develop axial cracks, which if not suppressed, will certain propagate. Non-barrier failures tended to develop local circumferential cracks, although some axial cracks have been observed. The alloy-barrier fuel tended to have moderate degradation at most; however, additional data is needed to form a conclusion as to the effectiveness of the alloy liner with respect to degradation resistance. One would expect that alloy liner fuel would degrade in a manner similar to that of non-barrier fuel, since the oxidation and presumably hydriding of alloy liner is not necessarily superior to that of Zr-2.

The evolution of degradation is dependent upon a number of variables, the most significant of which appears to be peak local power in conjunction with the axial power profile. Secondary degradation is indirectly dependent upon other variables such as: fuel design, location of the primary failure site, burnup, and time of operation.

The case studies support the conclusion that peak local power and axial power profile are the most significant factors affecting the evolution of secondary degradation. Among these three failures, one observes that the two failures (GE12 and GE11) with longer operating time developed small cracks as compared to bulges in the GE10. Therefore burnup is not considered a significant factor in degradation. The one 8x8 non-barrier case severely degraded within 14 days. The (9x9) GE11 alloy-barrier and 10x10 (S96) non-barrier cases developed significant hydriding near the peak power location, but the GE11 alloy-barrier failure did not degrade by circumferential fracture, whereas the non-barrier 10x10 failures did.

It is recommended that additional power history data be obtained in order to allow a better understanding of the effect of local power on the local degradation process. It is desirable to obtain power histories for those failures of a similar fuel (and cladding) design that have similar locations of the primary defect in order to understand the impact of local power and power distribution on the degradation process.

# A

# APPENDIX A: COMPARISON OF ALLOY-BARRIER AND BARRIER FAILURE DEGRADATION WITH THAT OF NON-BARRIER FAILURES

Comparison of Alloy-barrier and Barrier Failure Degradation with that of Non-Barrier Failures

In the S64 (8x8) population, the secondary degradation tended to be below the first spacer. The single alloy-liner failure (18701 G4) had hydriding at 19.7-inch elevation, which is similar to the location of 17.7-inch of one of the non-liner S64 failure (18834 C2). In contrast, the other S64 failure (20790 C7) suffered significant degradation at a lower elevation (11-14.6 inches). In this case degradation of the non-liner fuel was more severe than the alloy-liner fuel. This trend is surprising since the alloy-liner failure (18701) operated 197 days while the non-liner failure (20790) apparently degraded within approximately 14 days. It is likely the local and rod average power levels were the critical factors in the degradation.

In the S96/S100 population, the degradation of the three alloy-liner failures appears comparable to that of non-liner (non-barrier) fuel. With debris failures at the upper spacers, the secondary hydriding in the form of bulges and circumferential fractures is found generally between spacers 1 and 2 or below spacer 1. Coincidentally, alloy-liner failure AFB129 D7 and non-liner failure ADB073 A4 both have debris failures at the 108-inch elevation with secondary hydriding at 25 inches. The non-liner failure has a circumferential fracture at that location. Interestingly, the alloy-liner fuel operated 301 days as compared to 183 days for the non-liner failure. Generally, the location of secondary hydriding and breaches in the non-liner failures were not directly dependent of burnup and therefore, it is apparent that local power and the axial power distribution are the critical factors. This may also be true for the alloy-liner fuel, even though the population of alloy-liner fuel failures is too limited to derive such a conclusion.

The single Zr-Fe liner failure (GE11, IGE646 J4) operated approximately 231 days with 182 days of suppression. Although it operated for 53 days at high power (approximately 10.3 kW/ft). One explanation for the lack of degradation is the relatively low burnup of the fuel, which was approximately 0.3 GWD/MTU at failure, which occurred 14 days after startup. In this case, there was probably a sufficient gap between fuel and cladding to permit moisture along the fuel rod. After suppression, the gap would have remained open.

The degradation of non-liner and liner (pure Zr) for 9x9-9Q/-9QA is compared in Table A-2. With regard to failures that have similar locations of the primary defect, one observes that the secondary degradation tends to occur also at similar locations. KU0863 A3 (non-liner) and JB075K G1 (liner) both have debris fretting at spacer 4 (approximately 80 inches from the LEP) and secondary defects between spacer 1 and 2. KU0787 B7 and JB039K K9 have debris failures at spacer 5 (approximately 100 inches from the LEP) and secondary defects below spacer 1. On the other hand, JB039K developed a long axial split.

**Table A-1**
**Comparison of Degradation in Alloy-Liner Fuel and Non-liner Fuel of Similar Design**

| Assembly ID | Rod Location ABB/GE pos. | Cause of Failure | Fuel Design* | Disch. Burnup GWD/MTU | Primary def Location (inch) | Location of Secondary Defect(s)** - (inch) |
|---|---|---|---|---|---|---|
| 18701 | G4 / E2 | Debris | S64AL | 33.3 | 132.7 (Sp 6) | hyd 19.7 |
| 20790 | C7 / B6 | Debris | S64 | 14.5 | 111.7 (Sp 5) | cf (hyd) 11, cr 11-14.6 |
| 18834 | C2 / G6 | Debris | S64 | 19.2 | 110.2 (Sp 5) | hyd 17.7 |
| | | | | | | |
| AFB072 | H4 / G3 | Debris | S96+/L | 12.0 | 123 (Sp 6) | blg (sp 1/sp2) |
| AFB080 | I3 /H2 | Debris | S96+/L | 12.0 | 139 (Sp 7) | blg 45 (sp 2), crblg (below Sp 1) |
| AFB129 | D7 | Debris | S96+/L | 12.0 | 108 (Sp 5) | blg 25, crblg 4 |
| ACA026 | A3 / H10 | Debris | S96 | 8.8 | 108 (Sp 5) | cf 29 |
| ACA031 | J4 / G1 | Debris | S96 | 9.2 | 123 (Sp 6) | cf 32 |
| 21145 | E8 / C6 | Debris | S100 | 10.1 | 123 (Sp 5) | cf (LEP and sp 1) |
| ABA010 | C8 | Debris | S96 | 10.5 | 92 (Sp 4) | blgs below Sp 1 |
| ADB073 | A4 / G10 | Debris | S96 | 11.5 | 108 (Sp 5) | cf 25 |
| 20490 | G4 | Debris | S100 | 12.5 | 123 (Sp 5) | 15.4 above LEP |
| 20555 | H4 / G3 | Debris | S100 | 18.6 | 123 (Sp 5) | nothing (no secondary) |
| ACB116 | D5 / F7 | Debris | S96 | 19.1 | 108 (Sp 5) | cf 24 |
| 23014 | B10 / A9 | Debris | S96 | 22.7 | 103.1 (Sp 5) | hyd 36.7 |
| 19502 | H2/ J3, H3, I2/ J2, I3/ H2 | Debris | S100 | 22.8 | 0 (LEPW) | No significant degradation |
| 21965 | E2 / J6 | Debris | S96 | 23.2 | 118.1 (Sp 6) | hyd 43.3 |
| 18945 | J9 / B1 | Debris | S100 | 23.7 | 123 (Sp 6) | 6 in. crack below sp 1 |
| AEC092 | J6 / E1 | Debris | S96 | 24.8 | 108 (Sp 5) | cf (sp 1/sp2) |
| 21038 | I5 / F2 | Debris | S100 | 25.3 | 134.3 (Sp 6) | hyd 41.3 |
| 21007 | D2 / J7 | Debris | S100 | 28.7 | 133.5 (Sp 6) | hyd 36.7 |
| 21253 | F2 / J5 | Debris | S100 | 29.7 | 92 (Sp 4) | 2 in. below spacer 1 (crack) |
| AAA045 | B2 / J9 | Debris | S96 | 47.7 | 123 (Sp 6) | hyd 68-70 (Sp 3) |

*S64AL and S96+/L have Zr-Sn liner
** Description of secondary defects
cr =crack, cf = circ frac, blg = bulge, crblg = cracked bulge, bls = blister, hyd = hydride, ec = eddy-current indication

**Table A-2**
**Comparison of Degradation in Liner Fuel and Non-liner Fuel of Similar Design**

| Assembly ID | Rod Location pos. | Cause of Failure | Fuel Design* | Disch. Burnup GWD/MTU | Primary def Location (inch) | Location of Secondary Defect(s)* - (inch) |
|---|---|---|---|---|---|---|
| Non-liner | | | | | | |
| KU0863 | A3 | Debris | 9-9QA | 19.4 | 80 | axial crack between sp 1 and 2 |
| KU0787 | B7 | Debris | 9-9QA | 19.6 | 100 | small cf below sp 1 |
| KU0955 | G9 | Unk | 9-9QA | 21.4 | axial crack sp. 1 and 2 | lower end plug |
| KU0948 | A9 | Debris | 9-9QA | 29.3 | 120 | blgs, hole below sp 1 |
| KU0679 | B5 | Debris | 9-9QA | 35.7 | 20 | blg below sp 6 |
| Liner (pure Zr) | | | | | | |
| JB 075 K | G1 | Debris | 9-9QA | 8.2 | 80 | spiral cr 19.7-26, cr 26-30 |
| JB 039 K | K9 | Debris | 9-9QA | 11.8 | 98.5 | cr 23.6 - 61; bulges 11.4, 13.8, 15.5, 18.1 |
| KB 077 K | E2 | Debris | 9-9QA | 17.6 | unk | cr 26.8 -30.7; blg 23.6, 27.5, 96 |
| KB 019 K | F9 | Debris | 9-9QA | 18.3 | 120 | cr 18.4-100.4 |
| HA 144 K | F3 | Debris | 9-9Q | 27.4 | n/a | 9 in. cr |
| HA 082 K | D7 | Debris | 9-9Q | 33.0 | 0 | cr 126-127.5 |
| HA 067 K | C4 | Debris | 9-9Q | 35.9 | 0 | EC (inside) signals 137-149, blg 159 |
| HA 057 K | G7 | Debris | 9-9Q | 36.0 | 0 | cf 145 |
| HA 087 K | C6 | Debris | 9-9Q | 41.4 | 0 | n/a |
| HA 095 K | E2 | Debris | 9-9Q | 41.9 | 79 | No significant degradation |
| HA 095 K | G4 | Debris | 9-9Q | 41.9 | 0 | EC (inside) signals 126 above LEP |

* Description of secondary defects
cr =crack, cf = circ frac, blg = bulge, crblg = cracked bulge, bls = blister, hyd = hydride, ec = eddy-current indication

# B

# APPENDIX B: COMPARISON OF 8X8, 9X9 AND 10X10 FAILURES SORTED BY SEVERITY OF DEGRADATION

**Table B-1**
**Summary of 8x8 Failures Sorted by Severity of Degradation**

| Assembly ID | Rod Location (ABB)/ GE | Cause of Failure | Fuel Design | Burnup at Disch. GWD/MTU | Location of Primary Def (inch) | Location of Degradation (inch) cr =crack, cf = circ frac blg = bulge, crblg = cracked bulge bls = blister, hyd = hydride ec = eddy-current indication | Clad Type b=Zr iner ab =alloy-bar. nb =non-bar. | Deg. Cat. 4=severe 3=major 2=moder 1=minor x=not reported |
|---|---|---|---|---|---|---|---|---|
| 18701 | (G4)/ E2 | Debris | S64AL | 33.3 | 132.7 | 19.7 | ab | 2 |
| LYL284 | A6 | Mfg-Possible PCI | GE8B | 28.9 | Unk | ec 26-32 | b | 1 |
| YJ5168 | E1 | Unk - PCI? | GE9B | 33.26 | 55 | hyd 19 | b | 1 |
| LYL133 | E6 | Possible PCI | GE8B | 43.0 | n/a | cf 139; crblg 5, 6; blg 85, 105 | b | 2 |
| LYS488 | F8 | Debris | GE8B | 21.1 | 120 | blg 56 | b | 2 |
| LYT305 | B7 | Unk-Mfg | GE7B | 30.7 | Unk | blg 8; blg 42-47; hyd 159 (UEP) | b | 2 |
| KLG072 | B4 | Mfg | GE10 | 27.2 | 94 | X-mark 94-95; blg 16 | b | 2 |
| JM055 | E8 | Unk | 8-2L | 34.5 | | blg 69, 142 | b | 2 |
| LYG021 | F1 | Possible PCI | GE8B-4W | 28.1 | Unk | cr 137-138; crblg 3 | b | 2 |
| LYG035 | A4 | Possible PCI | GE8B-4W | 30.0 | Unk | blg 58; ec 6, 46,59 | b | 2 |
| LYJ916 | H4 | Unk-Mfg | GE8B | 37.0 | Unk | blgs 28, 94, 96, 141, 146 | b | 2 |
| LYJ855 | H4 | Unk-Mfg | GE8B | 36.4 | Unk | blgs 28, 30, 32 | b | 2 |
| LYJ855 | E8 | Unk-Mfg | GE8B | 36.4 | Unk | blgs 7, 11, 18,83, 85-100 | b | 2 |
| LYJ855 | G8 | Unk-Mfg | GE8B | 36.4 | Unk | blgs at 39, 59, 63,64,65, 118; crblg at 150 | b | 2 |
| CAC158 | H4 | Mfg | GE9B | 20.1 | ?85.8" | 25.9",28.7",31.5", 36" | b | 2 |
| YJ7372 | F1 | Debris | GE10 | 42.0 | 140 | blg 21, 66, 85, 92 | b | 2 |
| LYA459 | C3 | Possible PCI | GE7B | 26.8 | Unk | cr 30, cf 159 (UEP) | b | 3 |
| LYX155 | E3 | Debris | GE9B | 17.5 | 121.5 | cr 30-33 | b | 3 |
| YJ2263 | C4 | Mfg-LEPW | GE8B | 11.2 | 0 | cf 159 | b | 3 |
| LYH443 | A4 | Possible PCI | GE8B | 40.3 | Unk | cr 144.5-145.5; bls 2-55, 101-120 | b | 3 |
| JM064 | E2 | Debris | 8-2L | 27.9 | 20.5 | cf at UEP | b | 3 |
| YJ8371 | G2 | Debris | GE8B | 1.2 | 140 | cf 21 | b | 3 |
| LYG037 | A6 | Possible PCI | GE8B-4W | 27.9 | Unk | cr 140; ec 45, 43, 46, 140,142,144 | b | 3 |
| LYL294 | B2 | Unk-Debris | GE8B | 29.0 | Unk | blg 159, cf 159 (UEP) | b | 3 |
| LYJ855 | D2 | Unk-Mfg | GE8B | 36.4 | Unk | Circ crack at 100-116, | b | 3 |
| LYJ855 | F8 | Unk-Mfg | GE8B | 36.4 | Unk | crblgs at 121, 122; UEP bulge, circ. crack | b | 3 |
| LYZ621 | G4 | Unk | GE9B | 36.8 | Unk | cr 51, cr 78-81; blg 139 | b | 3 |
| YJ4932 | F6 | Unk | GE9B | 22.4 | Unk | cr 11-15 | b | 3 |
| YJ9760 | H7 | Debris | GE9B | 2.8 | 140 | cf 26, cf 28 | b | 3 |
| YJ8327 | A3 | PCI? | GE10 | 13.0 | Unk-22? | cr/cf 21-23.5 | b | 3 |
| YJB806 | B5 | Debris | GE10 | 26.5 | 140 | cr 70-74 | b | 3 |
| YJD643 | B3 | Unk-Debris? | GE9B | ~14 | Unk | cr / cf 25 - 30 | b | 3 |
| YJD636 | H3 | Debris | GE9B | 14.0 | 142 | cf 159 (UEP), cf (sp1-sp2) | b | 3 |
| LYP571 | D1 | Mfg-Possible PCI | GE8B | 29.6 | Unk | cr 28-40, cf 159 (UEP) | b | 4 |

**Table B-1 (continued)**
**Summary of 8x8 Failures Sorted by Severity of Degradation**

| Assembly ID | Rod Location (ABB)/ GE | Cause of Failure | Fuel Design | Burnup at Disch. GWD/MTU | Location of Primary Def (inch) | Location of Degradation (inch)<br>cr =crack, cf = circ frac<br>blg = bulge, crblg = cracked bulge<br>bls = blister, hyd = hydride<br>ec = eddy-current indication | Clad Type<br>b=Zr iner<br>ab =alloy-bar.<br>nb =non-bar. | Deg. Cat.<br>4=severe<br>3=major<br>2=moder<br>1=minor<br>x=not reported |
|---|---|---|---|---|---|---|---|---|
| LYX042 | C6 | Debris | GE9B | 17.4 | 79 | cr 19-28, cr 31-38, bls 16-50 | b | 4 |
| LYA232 | A4 | Possible PCI | GE7B | 24.4 | Unk | cr 30-34, cr 70-110 | b | 4 |
| LYH359 | A1 | PCI | GE8B | 41.9 | n/a | cr 90-110, cr 111; hyd 159; bl 40-80 | b | 4 |
| LYL122 | A5 | Possible PCI | GE8B | 43.8 | n/a | cr 78-99, cr 127-135; bl 127, bl 26-70 | b | 4 |
| KLG055 | F3 | Mfg | GE10 | 27.0 | 100 | cr 86-120(propagating primary); bl 7 | b | 4 |
| LYL250 | A6 | Mfg-Possible PCI | GE8B | 28.9 | Unk | cr 13.4-16.1, 16.5-17.5, 29.9-36 | b | 4 |
| YJ5835 | A3 | Debris | GE9B | 21.7 | 140 | cr 31-62, cr 62-112 | b | 4 |
| YJB787 | A6 | Unk | GE10 | 18.8 | Unk | cr 31-40, cr 40-115 | b | 4 |
| YJB856 | D1 | Debris | GE10 | ~26 | 120 | cr 51-114 | b | 4 |
| YJ8594 | D1 | Debris | GE10 | >30 | 120 | Multiple cracks 10-130 | b | 4 |
| LYA354 | B4 | Debris | GE7B | 26.8 | 1 | | b | x |
| KJ 007 | D6 | Unk | 8-2L | 14.3 | | | b | x |
| LYM759 | D4 | Debris | GE7B | 28.5 | 2 | n/a | b | x |
| n/a | n/a | Mfg | GE9B | 29.3 | n/a | n/a | b | x |
| n/a | n/a | Mfg | GE9B | 27.2 | n/a | n/a | b | x |
| LYX334 | n/a | No insp | GE10 | 21.1 | n/a | n/a | b | x |
| LYW211 | A8 | Debris | GE8B | 34.3 | 141 | | b | x |
| YJ5___ | n/a | Debris | GE9 | 33.0 | n/a | n/a | b | x |
| XNC-827 | B5 | Unk-debris, PCI | 8-2 | 26.3 | 60 | None | nb | 1 |
| KS2581 | F3 | Unk | 8-2 | ~30 | n/a | none | nb | 1 |
| 18834 | (C2) / G6 | Debris | S64 | 19.2 | 110.2 | 17.7 | nb | 2 |
| 20790 | (C7) / B6 | Debris | S64 | 14.5 | 111.7 | cf (hyd) 11, cr 11-14.6 | nb | 4 |
| 16263 | (H6) / C1 | PCI | S64 | 32.1 | | | nb | x |
| 16594 | (H6 )/ C1 | PCI-probable | S64 | 25.9 | | | nb | x |
| 17210 | G2 | PCI-probable | S64 | 25.7 | | | nb | x |
| 17267 | (D4?)/ E5 | Unk | S64 | 45.4 | | | nb | x |
| 17893 | | Debris | S64 | 39.0 | | | nb | x |
| 17136 | | Debris | S64 | 40.0 | | | nb | x |

**Table B-2**
**Summary of 9x9 Failures Sorted by Severity of Degradation**

| Assembly ID | Rod Location | Cause of Failure | Fuel Design | Burnup at Disch. GWD/MTU | Location of Primary Def (inch) | Location of Degradation (inch) cr =crack, cf = circ frac blg = bulge, crblg = cracked bulge bls = blister, hyd = hydride ec = eddy-current indication | Clad Type b=Zr iner ab =alloy-bar. nb =non-bar. | Deg. Cat. 4=severe 3=major 2=moder 1=minor x=not reported |
|---|---|---|---|---|---|---|---|---|
| IGE646 | J4 | Debris | GE11 | 7.2 | 80 | crblg 17, 18, 19; blg21, 23; hyd 24-28 | ab | 2 |
| HA 095 K | E2 | Debris | 9-9Q | 41.9 | 79 | No signficant degradation | b | 1 |
| HA 095 K | G4 | Debris | 9-9Q | 41.9 | 0 | EC (inside) signals 126 above LEP | b | 1 |
| HA 067 K | C4 | Debris | 9-9Q | 35.9 | 0 | EC (inside) signals 137-149, blg 159 | b | 2 |
| YJ2624 | G6 | Debris | GE11B | 20.4 | 140 | crblg at 21 | b | 2 |
| YJ2802 | C5 | Debris | GE11B | 23.1 | 140 | crblg at 77 | b | 2 |
| YJE016 | J8 | Debris | GE11B | 30.0 | 0 | cr 141 | b | 2 |
| HA 057 K | G7 | Debris | 9-9Q | 36.0 | 0 | cf 145 | b | 3 |
| HA 082 K | D7 | Debris | 9-9Q | 33.0 | 0 | cr 126-127.5 | b | 3 |
| KB 077 K | E2 | Debris | 9-9QA | 17.6 | unk | cr 26.8 -30.7; blg 23.6, 27.5, 96 | b | 3 |
| KD005K | A4 | Mfg-LEPW | GE11 | 9.0 | 0 | cr 144 (small) above Sp 7 | b | 3 |
| YJ7119 | B5 | Unk-Carryover | GE11B | 15.8 | Unk | cf at 0 (LEP), cr 23-26, cr 15-16, blg 30 | b | 3 |
| ND098K | E8 | Debris | GE11T | 7.0 | 80 | cr 21.7 | b | 3 |
| YJD180 | E7 | Debris | GE13 | 28.3 | 132 | cr 70-73 | b | 3 |
| JB 075 K | G1 | Debris | 9-9QA | 8.2 | 80 | spiral cr 19.7-26, cr 26-30 | b | 4 |
| JB 039 K | K9 | Debris | 9-9QA | 11.8 | 98.5 | cr 23.6 - 61; bulges 11.4, 13.8, 15.5, 18.1 | b | 4 |
| HA 144 K | F3 | Debris | 9-9Q | 27.4 | | 9 in. cr | b | 4 |
| UB013B | B7 | Mfg | GE11B | 5.2 | n/a | blg 17; cf 32, 35, 38; cr 39-59 | b | 4 |
| KB 019 K | F9 | Debris | 9-9QA | 18.3 | 120 | cr 18.4-100.4 | b | 4 |
| YJ1590 | G9 | Unk (Deb, mfg) | GE11B | 29.2 | n/a | crblg 6, 35; blg 8, 37; cr 65, 67-121 (spiral); cf 76 | b | 4 |
| A3W034 | H2 | Unk | 9-2L | 14.0 | unknown | cf ~12 | b | 4 |
| | | n/a | 9-9QA | n/a | | | b | x |
| HA 087 K | C6 | Debris | 9-9Q | 41.4 | 0 | | b | x |
| YJ2013 | G7 | Debris | GE10 | 26.4 | 140 | | b | x |
| YJA708 | A3 | Debris | GE11B | 15.0 | | | b | x |
| YJA721 | G7 | Debris | GE11B | 16.0 | | | b | x |
| | | n/a | 9-9QA | n/a | | | b | x |
| UB____ | | Mfg | GE11B | 41.0 | | | b | x |
| UB01HZ | n/a | n/a | GE11B | 39.2 | n/a | n/a | b | x |
| UB01GW | n/a | n/a | GE11B | 42.0 | n/a | n/a | b | x |
| HGE351 | F1 | CILC-II | GE11B | 17.0 | 52.5 | n/a | b | x |
| HGE351 | E1 | CILC-II | GE11B | 17.0 | 52.5 | n/a | b | x |
| HGE351 | A4 | CILC-II | GE11B | 17.0 | 52.5 | n/a | b | x |
| HGE352 | A4 | CILC-II | GE11B | 17.0 | 50 | n/a | b | x |
| HGE352 | A4 | CILC-II | GE11B | 17.0 | 50 | n/a | b | x |
| HGE352 | A4 | CILC-II | GE11B | 17.0 | 50 | n/a | b | x |
| HGE348 | H2 | CILC-II | GE11B | 17.0 | 33 | n/a | b | x |
| HGE339 | B2 | CILC-II | GE11B | 17.0 | 45-50 | n/a | b | x |
| HGE337 | Not Insp | CILC-II | GE11B | 17.0 | Not Insp | n/a | b | x |
| HGE340 | B2 | CILC-II | GE11B | 17.0 | 45 | n/a | b | x |
| HGE322 | Not Insp | CILC-II | GE11B | 17.0 | Not Insp | n/a | b | x |
| ND099 K | ?? | No insp yet | GE11T | 22 | | No insp yet | b | x |

*Appendix B: Comparison of 8x8, 9x9 and 10x10 Failures Sorted by Severity of Degradation*

**Table B-2(continued)**
**Summary of 9x9 Failures Sorted by Severity of Degradation**

| Assembly ID | Rod Location | Cause of Failure | Fuel Design | Burnup at Disch. GWD/MTU | Location of Primary Def (inch) | Location of Degradation (inch)<br>cr =crack, cf = circ frac<br>blg = bulge, crblg = cracked bulge<br>bls = blister, hyd = hydride<br>ec = eddy-current indication | Clad Type<br>b=Zr iner<br>ab =alloy-bar.<br>nb =non-bar. | Deg. Cat.<br>4=severe<br>3=major<br>2=moder<br>1=minor<br>x=not reported |
|---|---|---|---|---|---|---|---|---|
| AND018 | A2 | Unk-debris, PCI | 9-5 | 14.7 | 130-133 | None | nb | 1 |
| AND122 | A5 | Unk-debris, PCI | 9-5 | 15.2 | 81-83 | None | nb | 1 |
| AND043 | B4 | Debris | 9-5 | 22.1 | 140 | None | nb | 1 |
| KAA119 | K3 | Debris | 9-2 | 27.0 | n/a | none | nb | 1 |
| SPF767 or 768 | n/a | No exam | 9-5 | ~26 | n/a | none | nb | 1 |
| X24885 | C9 | Unk | 9-2 | 23.2 | Unknown | 25",70",135" | nb | 2 |
| KU0679 | B5 | Debris | 9-9QA | 35.7 | 20 | blg below sp 6 | nb | 2 |
| KU0787 | B7 | Debris | 9-9QA | 19.6 | 100 | small cf below sp 1 | nb | 3 |
| KU0863 | A3 | Debris | 9-9QA | 19.4 | 80 | axial crack between sp 1 and 2 | nb | 3 |
| KU0955 | G9 | Unk | 9-9QA | 21.4 | cr around sp. 1 and 2 | lower end plug | nb | 3 |
| KU0948 | A9 | Debris | 9-9QA | 29.3 | 120 | blgs, hole below sp 1 | nb | 3 |
| CA 162 K | A9 | Debris | 9-5 | 35-40 | | | nb | x |
| 0519 | | Unk, PCI? | 9-1 | 30.9 | | | nb | x |
| | | n/a | 9-5 | 38.8 | | | nb | x |
| 0668 | A5 | PCI | 9-1 | 30.2 | | | Nb | x |
| 0769 | C1 | PCI | 9-1 | 29.2 | | | nb | x |
| | | | 9-1 | 16.1 | | | nb | x |
| 0578 | C1 | Unk, PCI? | 9-1 | 30.4 | | | nb | x |
| 0823 | | Unk, PCI? | 9-1 | 34.8 | | | nb | x |
| | | ? | 9-1 | | | | nb | x |

**Table B-3**
**Summary of 10x10 Failures Sorted by Severity of Degradation**

| Assembly ID | Rod Location | Cause of Failure | Fuel Design | Burnup at Disch. GWD/MTU | Location of Primary Def (inch) | Location of Degradation (inch)<br>cr =crack, cf = circ frac<br>blg = bulge, crblg = cracked bulge<br>bls = blister, hyd = hydride<br>ec = eddy-current indication | Clad Type<br>b=Zr iner<br>ab =alloy-bar.<br>nb =non-bar. | Deg. Cat.<br>4=severe<br>3=major<br>2=moder<br>1=minor<br>x=not reported |
|---|---|---|---|---|---|---|---|---|
| AFB072 | (H4)/ G3 | Debris | S96+/L | 12.0 | 123 | blg (sp 1/sp2) | ab | 2 |
| AFB080 | (I3)/H2 | Debris | S96+/L | 12.0 | 139 | blg 45 (sp 2), crblg (below Sp 1) | ab | 2 |
| AFB129 | D7 | Debris | S96+/L | 12.0 | 108 | blg 25, crblg 4 | ab | 2 |
| MA005 | (E2) / J6 | Debris | S96AL | 11.0 | | | ab | x |
| MA017 | (B1) / K9 | Debris | S96AL | 12.0 | | | ab | x |
| LD062 | (F2) / J5 | Debris | S96AL | 12.0 | | | ab | x |
| LC010 | (H7) / D3 | Debris | S96AL | 19.0 | | | ab | x |
| LB031 | (E4) / G6 | Debris | S96AL | 20.0 | | | ab | x |
| | | Debris | S96AL | ~20 | | | ab | x |
| | | Debris | S96AL | ~20 | | | ab | x |
| | | Debris | S96AL | | | | ab | x |
| YJK861 | J6 | Debris | GE12B | 15.0 | 82 | cr 23-24, crblg 20, blg 10, 11 | b | 3 |
| 20555 | (H4) / G3 | Debris | S100 | 18.6 | 133 | nothing (no secondary) | nb | 1 |
| AAA045 | (B2) / J9 | Debris | S96 | 47.7 | 123 | hyd 68-70 (Sp 3) | nb | 1 |
| ABA010 | C8 | Debris | S96 | 10.5 | 92 | blgs below Sp 1 | nb | 2 |
| 21038 | (I5) / F2 | Debris | S100 | 25.3 | 134.3 | 41.3 | nb | 2 |
| 21007 | (D2) / J7 | Debris | S100 | 28.7 | 133.5 | 36.7 | nb | 2 |
| 21965 | (E2) / J6 | Debris | S96 | 23.2 | 118.1 | 43.3 | nb | 2 |
| 23014 | (B10)/ A9 | Debris | S96 | 22.7 | 103.1 | 36.7 | nb | 2 |
| 18945 | (J9) / B1 | Debris | S100 | 23.7 | 133 | 6 in. crack below sp 1 | nb | 3 |
| ACA026 | (A3)/H10 | Debris | S96 | 8.8 | 108 | cf 29 | nb | 3 |
| ACA031 | (J4) / G1 | Debris | S96 | 9.2 | 123 | cf 32 | nb | 3 |
| 21145 | (E8) / C6 | Debris | S100 | 10.1 | 133 | cf (LEP and sp 1) | nb | 3 |
| 21253 | (F2) / J5 | Debris | S100 | 29.7 | 88 | 2 in. below spacer 1 (crack) | nb | 3 |
| ACB116 | (D5) / F7 | Debris | S96 | 19.1 | 108 | cf 24 | nb | 4 |
| ADB073 | (A4)/G10 | Debris | S96 | 11.5 | 108 | cf 25 | nb | 4 |
| AEC092 | (J6) / E1 | Debris | S96 | 24.8 | 108 | cf (sp 1/sp2) | nb | 4 |
| 20490 | G4 | Debris | S100 | 12.5 | 133 | 15.4 above LEP | nb | 3,2 |
| S211 | (H5)/ F3 | Debris | S96 | 20.2 | | | nb | x |
| 17790 | (G3) / H4 | Debris | S100 | 24.3 | 87.8 | | nb | x |
| U211 | (G10)/A4 | Debris | S96 | 6.5 | | | nb | x |
| 17684 | (G6) / E4 | Debris | S100 | 32.3 | | | nb | x |
| 20224 | (I3) / H2 | Debris | S100 | 11.0 | | | nb | x |
| 19502 | (H2) / J3 | Debris | S100 | 22.8 | 0 | | nb | x |
| 19502 | H3 | Debris | S100 | 22.8 | 0 | | nb | x |
| 19502 | (I2) / J2 | Debris | S100 | 22.8 | 0 | | nb | x |
| 19502 | (I3) / H2 | Debris | S100 | 22.8 | 0 | | nb | x |
| ABB002 | ? | No exam | S96 | | | | nb | x |
| AAA038 | (E4 / G6 | ESSC or Debris | S96 | 54.2 | 69? | | nb | x |
| ABB066 | (C7) / D8 | ESSC or Debris | S96 | 47.3 | 69? | | nb | x |
| ABB075 | (A6)/ E10 | ESSC or Debris | S96 | 46.4 | 69? | | nb | x |
| ABB076 | (B8) / C9 | ESSC or Debris | S96 | 48.5 | 69? | | nb | x |
| 20681 | (J10) / A1 | Debris | S100 | 32.3 | | | nb | x |
| 21186 | | Not yet insp. | S100 | 31.0 | | | nb | x |
| ABA010 | (J1) / K10 | Unk-corrosion? | S96 | 44.0 | n/a | | nb | x |
| ABA010 | (F4) / G5 | Unk-corrosion? | S96 | 44.0 | n/a | | nb | x |
| | | Debris | A-10 | | | | nb | x |
| | | Debris | A-10 | | | | nb | x |

**About EPRI**

EPRI creates science and technology solutions for the global energy and energy services industry. U.S. electric utilities established the Electric Power Research Institute in 1973 as a nonprofit research consortium for the benefit of utility members, their customers, and society. Now known simply as EPRI, the company provides a wide range of innovative products and services to more than 1000 energy-related organizations in 40 countries. EPRI's multidisciplinary team of scientists and engineers draws on a worldwide network of technical and business expertise to help solve today's toughest energy and environmental problems.

EPRI. Powering Progress



1000692

*Printed on recycled paper in the United States of America*

EPRI • 3412 Hillview Avenue, Palo Alto, California 94304 • PO Box 10412, Palo Alto, California 94303 • USA
800.313.3774 • 650.855.2121 • askepri@epri.com • www.epri.com